AD-A159 924 3HE NUCLEAR GYROSCOPE(U) FRANK J SEILER RESEARCH LAB UNITED STATES AIR FORCE ACADEMY CO G L SHAW AUG 85 FJSRL-TR-85-0003 1/1

UNCLASSIFIED F/G 17/7 NL

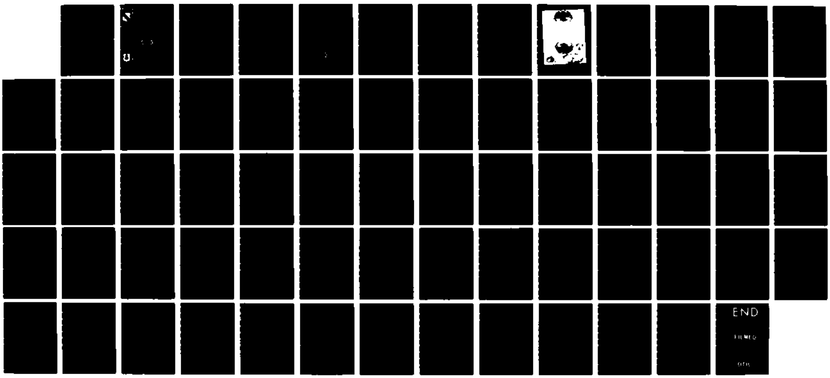

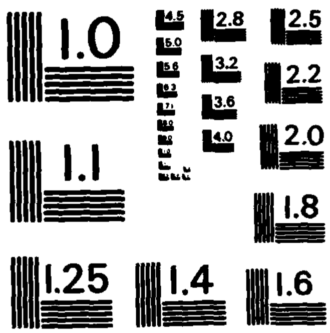


MICROCOPY RESOLUTION TEST CHART
NATIONAL BUREAU OF STANDARDS-1963-A

2



# FRANK J. SEILER RESEARCH LABORATORY

FJSRL-TR-85-0003 AUGUST 1985

## $^{3}$He NUCLEAR GYROSCOPE

FINAL REPORT



MAJOR GERALD L. SHAW

PROJECT 2301-F1-69





AIR FORCE SYSTEMS COMMAND

UNITED STATES AIR FORCE

FJSRL-TR-85-0003

This document was prepared by the Guidance and Control Division, Directorate of Lasers and Aerospace Mechanics, Frank J. Seiler Research Laboratory, United States Air Force Academy, Colorado Springs, CO. The research was conducted under Project Work Unit Number 2301-F1-69, Nuclear Gyroscopes. Major Gerald L. Shaw was the Project Scientist in charge of the work.

When U.S. Government drawings, specifications or other data are used for any purpose other than a definitely related government procurement operation, the government thereby incurs no responsiblity nor any obligation whatsoever, and the fact that the government may have forumulated, furnished or in any supplied the said drawings, specifications or other data is not to be regarded by implication or otherwise, as in any manner licensing the holder or any other person or corporation or conveying any rights or permission to manufacture, use or sell any patented invention that may in any way be related thereto.

Inquiries concerning the technical content of this document should be addressed to the Frank J. Seiler Research Laboratory (AFSC), FJSRL/NH, USAF Academy, Colorado Springs, CO 80840-6528. Phone AC 303 472-3122.

This report has been reviewed by the Commander and is releasable to the National Technical Information Service (NTIS). At NTIS it will be available to the general public, including foreign nations.

This technical report has been reviewed and is approved for publication.

Gerald L. Shaw

GERALD L. SHAW, Major, USAF
Project Scientist

Albert J. Alexander

ALBERT J. ALEXANDER, Major, USAF
Director, Lasers & Aerospace Mech

John H. Pletcher Jr.

JOHN H. PLETCHER, JR., Lt Col, USAF
Commander

Copies of this report should not be returned unless return is required by security considerations, contractual obligations, or notice on a specific document.

Printed in the United States of America. Qualified requestors may obtain additional copies from the Defense Technical Information Center. All others should apply to: National Technical Information Service
6285 Port Royal Road
Springfield, Virginia 22161

UNCLASSIFIED

SECURITY CLASSIFICATION OF THIS PAGE

# REPORT DOCUMENTATION PAGE

| | |
|---|---|
| 1a. REPORT SECURITY CLASSIFICATION<br>UNCLASSIFIED | 1b. RESTRICTIVE MARKINGS |
| 2a. SECURITY CLASSIFICATION AUTHORITY | 3. DISTRIBUTION/AVAILABILITY OF REPORT<br>Approved for public release; Distribution unlimited |
| 2b. DECLASSIFICATION/DOWNGRADING SCHEDULE | |
| 4. PERFORMING ORGANIZATION REPORT NUMBER(S)<br>FJSRL-TR-85-0003 | 5. MONITORING ORGANIZATION REPORT NUMBER(S) |
| 6a. NAME OF PERFORMING ORGANIZATION<br>Frank J. Seiler Research Lab<br>6b. OFFICE SYMBOL (If applicable)<br>FJSRL/NHG | 7a. NAME OF MONITORING ORGANIZATION |
| 6c. ADDRESS (City, State and ZIP Code)<br>USAF Academy<br>Colorado Springs, Colorado 80840-6528 | 7b. ADDRESS (City, State and ZIP Code) |
| 8a. NAME OF FUNDING/SPONSORING ORGANIZATION<br>8b. OFFICE SYMBOL (If applicable) | 9. PROCUREMENT INSTRUMENT IDENTIFICATION NUMBER |
| 8c. ADDRESS (City, State and ZIP Code) | 10. SOURCE OF FUNDING NOS. |

| PROGRAM ELEMENT NO. | PROJECT NO. | TASK NO. | WORK UNIT NO. |
|---|---|---|---|
| 61120F | | 2301-F1 | 69 |

11. TITLE (Include Security Classification)
$^3$He Nuclear Gyroscope (U)

12. PERSONAL AUTHOR(S)
Gerald L. Shaw

| 13a. TYPE OF REPORT | 13b. TIME COVERED | 14. DATE OF REPORT (Yr., Mo., Day) | 15. PAGE COUNT |
|---|---|---|---|
| Final | FROM Nov 80 to Jul 85 | 1985 August | 68 |

16. SUPPLEMENTARY NOTATION

17. COSATI CODES

| FIELD | GROUP | SUB. GR. |
|---|---|---|
| 2303 | 2310 | 1707 |
| | | |

18. SUBJECT TERMS (Continue on reverse if necessary and identify by block number)
cryogenic inertial instruments, inertial navigation, nuclear gyroscope, guidance and control.

19. ABSTRACT (Continue on reverse if necessary and identify by block number)

The $^3$He nuclear gyroscope is a single species cryogenic device which can be instrumented as a three degree of freedom gyroscope. Sensitivities to dynamic terms can be modeled, measured, and compensated by generation of cross axis magnetic fields. The magnetic field generation scheme is the equivalent of putting the gyro on a stabilized platform but requires no moving parts. Such a gyroscope would be most useful integrated with other cryogenic instruments in a high accuracy all cryogenic inertial measurement unit.

| | |
|---|---|
| 20. DISTRIBUTION/AVAILABILITY OF ABSTRACT<br>UNCLASSIFIED/UNLIMITED ☐ SAME AS RPT. ☒ DTIC USERS ☐ | 21. ABSTRACT SECURITY CLASSIFICATION<br>UNCLASSIFIED |
| 22a. NAME OF RESPONSIBLE INDIVIDUAL<br>GERALD L. SHAW, Major, USAF | 22b. TELEPHONE NUMBER (Include Area Code)<br>(303) 472-3122<br>22c. OFFICE SYMBOL<br>FJSRL/NH |

DD FORM 1473, 83 APR EDITION OF 1 JAN 73 IS OBSOLETE.

UNCLASSIFIED

SECURITY CLASSIFICATION OF THIS PAGE

TABLE OF CONTENTS

## LIST OF FIGURES

# I.0 INTRODUCTION

Nuclear magnetic resonance (NMR) gyro developments over the last 20 years have been aimed at providing a low cost, high reliability alternative to conventional mechanical gyroscopes. By removing the need for precision moving parts such devices would be inherently insensitive to mechanical shock and vibration; and thus well suited to strapdown systems. Two major NMR gyro developments in the United States produced engineering models which demonstrated rate bias stabilities of better than 1 deg/hr[1,2]. The goals for these devices ranged from 0.1 deg/hr to 0.01 deg/hr. However, the success of the laser gyro, which was aimed at the same market, caused abandonment of both of these NMR gyro programs.

For high accuracy applications, it has long been recognized that conventional inertial navigation system technology has advanced to the point where uncertainties in the knowledge of the earth's shape and gravity field represent significant sources of navigational error[3]. Thus, efforts are underway to develop gravity gradiometers for incorporation in high accuracy inertial measurement units. A room temperature gravity gradiometer has completed its initial sea trials and demonstrated an improved on-line measurement of the gravity gradient. This improved measure of gravitational acceleration will reduce the error for the deduced inertial acceleration; and the next generation inertial measurement unit, incorporating such a device, may well provide improved resolution using room temperature technology. However, potential advances possible with cryogenic instruments may well exceed any room temperature technology in the years ahead.

To realize the advantage possible with any one cryogenic instrument requires development of an entire family of cryogenic inertial instruments, since all must be integrated onto a single isothermal platform. Stanford University is developing the technology base to support both cryogenic gravity gradiometers and cryogenic accelerometers. The $^{3}$He nuclear gyro, the subject of this report, is the candidate gyro for such an all cryogenic inertial measurement unit. Stanford University has recently designed and constructed an all fused quartz $^{3}$He gyro housing consistent with a single axis angular stability approaching $2\times10^{-5}$ deg/hr (Figure 1-1).

## 2.0 BASIC PRINCIPLES

The $^{3}$He nucleus possesses both intrinsic spin angular momentum and a magnetic dipole moment which is directed antiparallel to the spin axis. However, a sample of $^{3}$He will not generally possess any net angular momentum or magnetization due to the random orientation of the individual spins. The process of optical pumping[4] is employed to orient the individual spins along a preferred direction and thus achieve a net sample angular momentum.

When such a polarized sample is placed in a uniform magnetic field, $\vec{B}$, two processes ensue. The first is a relaxation of the sample back to its unpolarized equilibrium condition (assuming the optical pumping process is terminated). The equilibrium value, $\vec{M}_o$, is determined using Boltzmann statistics to be

$$M_o = N|\vec{\mu}|\tanh \frac{|\vec{\mu}||\vec{B}|}{K_B T} \qquad (2\text{-}1)$$

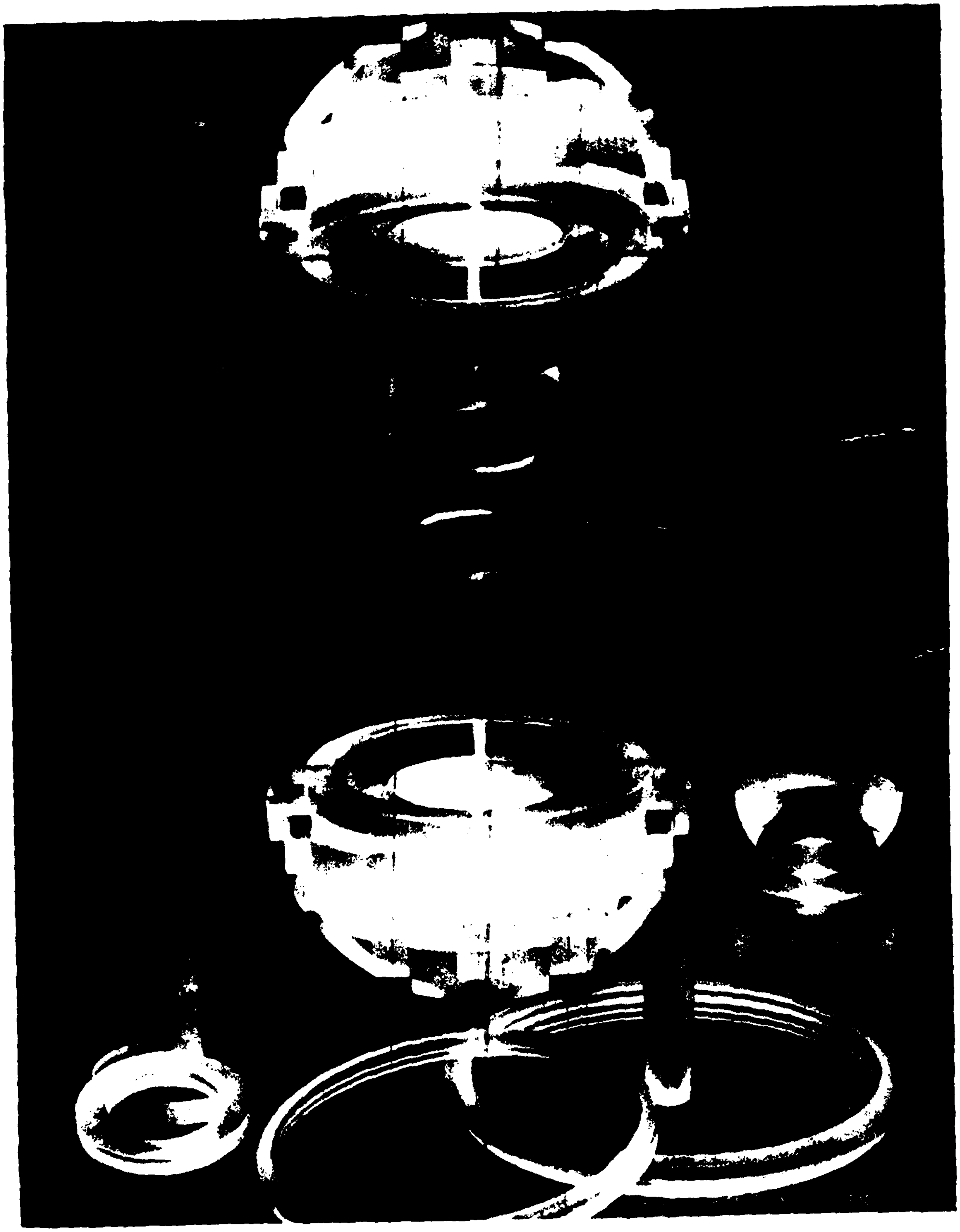

Figure 1-1. Fused Quartz $^3$He Nuclear Gyro Assembly

Where N is the number of $^3He$ atoms, $\vec{\mu}$ is the $^3He$ magnetic dipode moment, $k_B$ is Boltzmann's constant and T is the temperature. At equilibrium the net polarization lies along the applied field direction. Given that the equilibrium condition is approached at a rate proportional to the displacement from equilibrium, the relaxation process can be described by the differential equation

$$\frac{d}{dt}\begin{bmatrix} M_x \\ M_y \\ M_z \end{bmatrix} = \begin{bmatrix} -\frac{1}{T_2} & 0 & 0 \\ 0 & -\frac{1}{T_2} & 0 \\ 0 & 0 & -\frac{1}{T_1} \end{bmatrix}\begin{bmatrix} M_x \\ M_y \\ M_z \end{bmatrix} + \begin{bmatrix} 0 \\ 0 \\ \frac{m_o}{T_1} \end{bmatrix} \qquad (2\text{-}2)$$

where it is assumed that the applied field is in the $\hat{z}$ direction. The characteristic time $T_1$ is referred to as the longitudinal relaxation time and $T_2$ is the transverse relaxation time. $T_1$ and $T_2$ may be nearly equal; but, in general $T_1$ is greater because of magnetic field gradient effects.

The second process is due to the applied field interacting with the sample magnetization to produce a torque, $\vec{M} \times \vec{B}$. This torque equates to the time rate of change of the sample angular momentum in an inertial frame:

$$\frac{d}{dt}\vec{H} = \vec{M} \times \vec{B} \qquad (2\text{-}3)$$

But, $\vec{H}$ and $\vec{M}$ are antiparallel and in fact are related by the gyromagnetic ratio, $\gamma$, which is a constant for the species.

$$\vec{M} = \gamma\vec{H} \tag{2-4}$$

Thus the equation of motion can be written solely in terms of $\vec{M}$:

$$\frac{d}{dt}\vec{M} = \vec{M} \times \gamma\vec{B} \tag{2-5}$$

This equation holds for an inertial frame: but $\vec{B}$ is tied to the gyro. Then if the rotation rate of the gyro, with respect to the inertial frame, is $\vec{\omega}$, the equation of motion in the gyro frame is:

$$\frac{d}{dt}\vec{M} = \vec{M} \times \gamma\vec{B} - \vec{\omega} \times \vec{M} \tag{2-6}$$

$$= \vec{M} \times (\gamma\vec{B} + \vec{\omega}) \tag{2-7}$$

Then combining equations (2) and (7), with $\vec{B}$ still assumed to lie in the $\hat{z}$ direction, yields

$$\frac{d}{dt}\begin{bmatrix} M_x \\ M_y \\ M_z \end{bmatrix} = \begin{bmatrix} -\frac{1}{T_2} & (\gamma B+\omega_z) & -\omega_y \\ -(\gamma B+\omega_z) & -\frac{1}{T_2} & \omega_x \\ \omega_y & -\omega_x & -\frac{1}{T_1} \end{bmatrix} \begin{bmatrix} M_x \\ M_y \\ M_z \end{bmatrix} + \begin{bmatrix} 0 \\ 0 \\ \frac{m_o}{T_1} \end{bmatrix} \tag{2-8}$$

For a liquid sample of $^3He$ in $^4He$, a $T_2$ of greater than 140 hours has been obtained[5]. In principle $T_2$ can be made on the order of weeks. Thus for many calculations the relaxation effects are neglected leaving

$$\frac{d}{dt}\begin{bmatrix} M_x \\ M_y \\ M_z \end{bmatrix} = \begin{bmatrix} 0 & (\gamma B+\omega_z) & -\omega_y \\ -(\gamma B+\omega_z) & 0 & \omega_x \\ \omega_y & -\omega_x & 0 \end{bmatrix} \begin{bmatrix} M_x \\ M_y \\ M_z \end{bmatrix} \tag{2-9}$$

This equation is the basis of the nuclear gyro. The solution indicates that $\vec{M}$ precesses about an axis $-(\gamma\vec{B}+\vec{\omega})$ at a rate of $[(\gamma B+\omega_z)^2+\omega_x^2+\omega_y^2]^{1/2}$ rad/sec. Since $\gamma$ is a constant for a given nuclear species, the Larmor precession frequency, $\gamma B$, can be predicted. Any deviation from the Larmor rate is assumed to be due to a non-zero $\vec{\omega}$. Equation (9) shows that the greatest sensitivity of the gyro occurs for rotations in the $\hat{z}$-direction; but it is also clear that there is a mechanism to sense cross axis rates as well.

In order to utilize these principles in a practical device requires several elements. The first is a nuclear species, with intrinsic spin angular momentum. Ideally the species should be a spin 1/2 species; otherwise it will possess an electric quadrupole moment. An electric quadrupole moment is due to the ellipticity of the distribution of charge in the nucleus. The important point is that such a moment will interact with an electric field gradient to produce a torque on the nucleus, leading to a shift of the Larmor frequency. A spin 1/2 species, however, has only a magnetic dipole moment; and thus the only interaction of concern will be with a magnetic field. $^3He$ is such a species. It also has the added advantage of being useable as either a liquid or a gas at cryogenic temperatures, and demonstrates very long relaxation times.

The second element required is a means of polarizing the nuclear species. Optical pumping has been successfully employed on $^3He$ at room temperature[4]. A gas $^3He$ sample, polarized at room temperature, can be condensed in solution with $^4He$ without significant loss of polarization[5].

The third element is an applied magnetic field. One obvious difficulty in making a practical $^3He$ nuclear gyro is in obtaining a uniform, static magnetic field. The magnitude of the earth's magnetic field is on the order of 0.5G ($5 \times 10^{-5}$T) at the surface, and varies in magnitude and direction from one location to another. So one task is to screen the $^3He$ sample from ambient magnetic fields. A method has been developed to create low field, $10^{-8}$G ($10^{-12}$T), regions within a superconducting lead foil shield[6]. This type of shield has the property of perfect diamagnetism. That is, beyond a penetration depth, which is small compared to the foil thickness, the magnetic flux density in the foil is zero. Thus changing magnetic field environments external to the foil have absolutely no effect within the shielded region.

In addition to shielding from outside magnetic fields, a high degree of uniformity is required of the applied magnetic field. If sixth order superconducting Helmholtz coils are used to generate the applied field, the field gradiants will be largely due to inhomogeneities in the field trapped within the lead foil shield. Based on current capabilities for establishing ultra-low field regions, the major field inhomogeneity is estimated to be a linear gradient of magnitude less than $10^{-8}$ G-cm$^{-1}$ ($10^{-10}$ T-m$^{-1}$)[6]. Figure 2-1 shows a three axis magnetic field profile of an ultra-low field trapped within a 20 cm diameter lead foil shield[6]. Furthermore, the field generating coils can be made superconducting so that the applied field will be generated a persistent supercurrent, which is inherently very stable.

The remaining element of the $^3$He nuclear gyro is the readout mechanism. A sensitive magnetometer is required to monitor the precessing magnetization vector. Since there is already a requirement to maintain the shield and the field coils at cryogenic temperatures, a natural candidate for the magnetometer is the SQUID (Superconducting Quantum Interference Device) magnetometer. Fortunately this is also the most sensitive magnetometer currently available. Theory and use of the SQUID are described in a number of references[7,8,9,10]; SQUID use for a $^3$He nuclear gyro has been described by Taber[5].

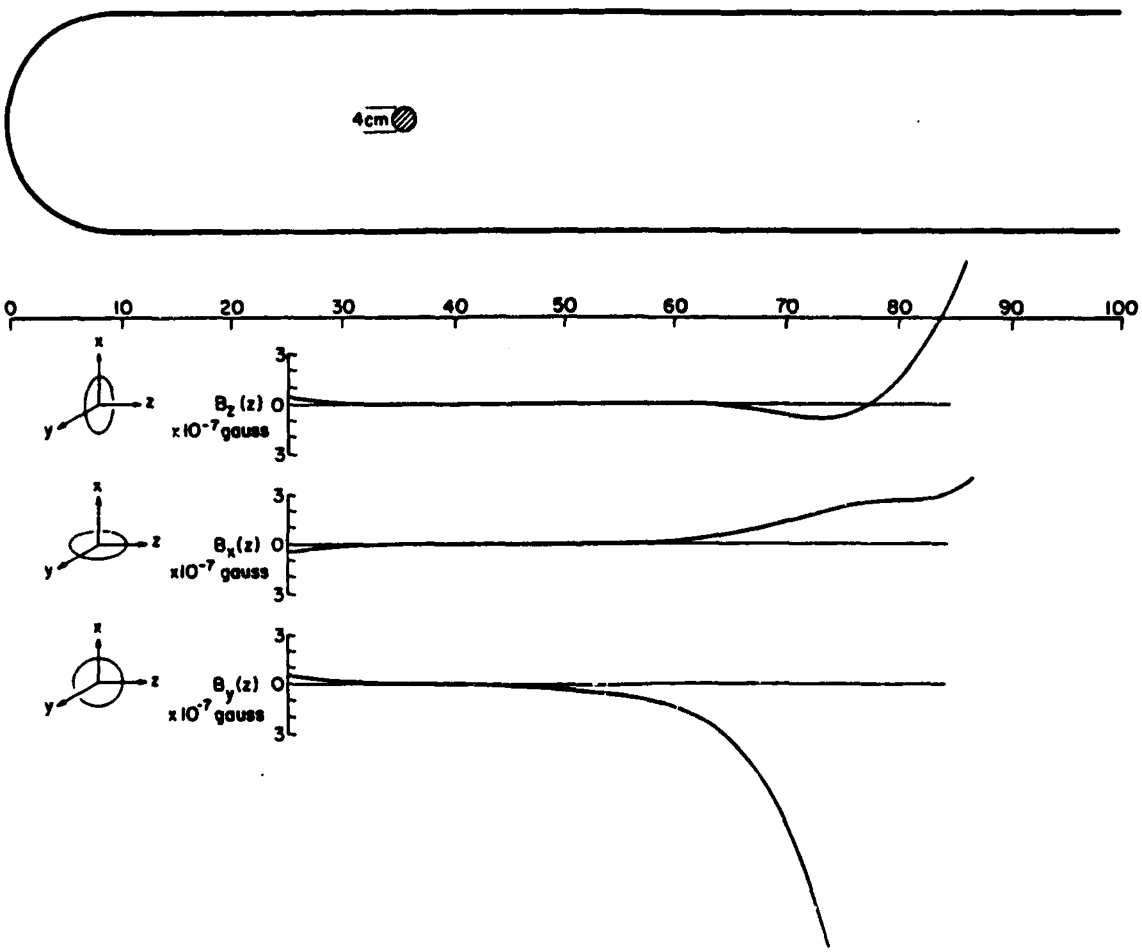


Figure 2-1. Three Mutually Perpendicular Magnetic Field Component Profiles Along the Axis of a 20 cm Diameter Super-conducting Shied

## 3.0 CROSS COUPLING EFFECTS

It is clear from Equation (2-9) that the nuclear gyro is not a true single degree of freedom gyro. Indeed, while the axis along the applied field has the greatest sensitivity, the device is affected by cross axis rates as well[11]. So, while we are trying to measure $\omega_z$, the instrument is sensitive to $\omega_x$ and $\omega_y$ also. Take, for example, the case where $\omega_x = \omega_z = 0$ and $\omega_y$ 0 then solving Equation (2-9) yields the following

$$\begin{bmatrix} M_x(t) \\ M_y(t) \\ M_z(t) \end{bmatrix} = \begin{bmatrix} \cos \omega t & \frac{\gamma B}{\omega} \sin \omega t & -\frac{\omega_y}{\omega} \sin \omega t \\ -\frac{\gamma B}{\omega} \sin \omega t & \cos \omega t + \left(\frac{\omega_y}{\omega}\right)^2 (1-\cos \omega t) & \frac{\gamma B \omega_y}{\omega^2} (1-\cos \omega t) \\ \frac{\omega_y}{\omega} \sin \omega t & \frac{\gamma B \omega_y}{\omega^2} (1-\cos \omega t) & \cos \omega t + \left(\frac{\gamma B}{\omega}\right)^2 (1-\cos \omega t) \end{bmatrix} \begin{bmatrix} M_x(0) \\ M_y(0) \\ M_z(0) \end{bmatrix} \quad (3\text{-}1)$$

where

$$\omega = \sqrt{(\gamma B)^2 + \omega_y^2} \; .$$

One effect of a cross axis input is immediately apparent. Even with no component of rotation about the applied field (input) axis, the precession frequency is $\sqrt{(\gamma B)^2 + \omega_y^2}$ rad/sec. This must be accounted for somehow to avoid a gyro drift error on the order of $1/2\ (\omega_y^2/\gamma B)$ rad/sec.

Figure 3-1 shows the effect of an uncorrected cross axis input. As shown above the drift grows as $\omega_y^2$ and inversely with the Larmor frequency, $\gamma B$. This suggests that cross coupling effects can be made arbitrarily small simply by increasing B. However, for a cross axis input rate of 1.0 rad/sec, the Larmor frequency must be $10^7$ rad/sec to reduce the uncorrected drift to $5 \times 10^{-8}$ rad/sec (0.01 deg/h). For $He^3$ this requires that B be about 490 G ($4.9 \times 10^{-2}$T). The gradients associated with such large fields make them impractical. The better approach is to measure the cross axis inputs and then compensate for their effects.

So consider the general case where there is both an input axis and a cross axis component of the input rate. Take the two respective components of $\vec{\omega}$ to be $\omega_z$ and $\omega_y$. There is no loss of generality here since the direction of the Y-axis, in the plane normal to the Z-axis, is arbitrary. Proceeding as before, we get

$$\frac{d}{dt}\vec{M} = \begin{bmatrix} 0 & (\gamma B + \omega_z) & -\omega_y \\ -(\gamma B + \omega_z) & 0 & 0 \\ \omega_y & 0 & 0 \end{bmatrix} \vec{M} \qquad (3\text{-}2)$$

The solution is thus the same as (3.1) with the term $\gamma B$ replaced by $(\gamma B + \omega_z)$. Thus the precession frequency seen in the gyro frame is now $\gamma[(B + \omega_z/\gamma)^2 + (\omega_y/\gamma)^2]^{1/2}$. It can also be shown that the normal to the tip path plane (precession plane) of $\vec{M}$ is parallel to $\gamma(B + \omega_z/\gamma)$ $z + \gamma(\omega_y/\gamma)\hat{Y}$. That is the behavior which is identical to the case where $\omega = 0$ and the applied field is

$$\vec{B} = (B + \frac{\omega_z}{\gamma})\hat{z} + (\frac{\omega_y}{\gamma})\hat{Y}.$$

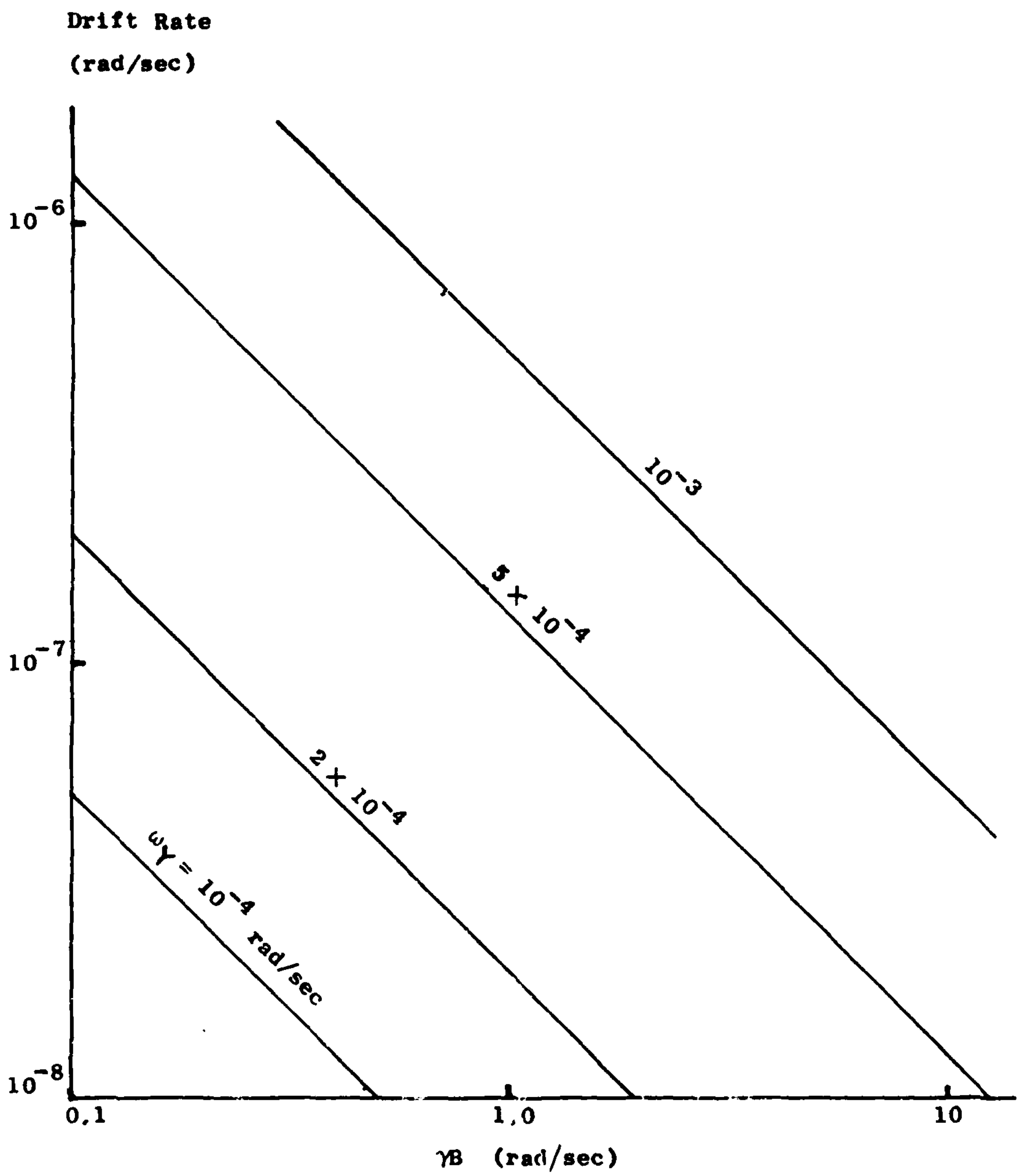


Figure 3-1. Drift Rate vs. Larmor Frequency for a Number of Cross Axis Input Rates, $\omega_Y$.

where $\hat{Z}$ and $\hat{Y}$ are unit vectors along the Z and Y axes respectively. This is simply a statement of the equivalence between rotations and magnetic fields[12]. Thus the effect of a cross axis rotation, $\omega_y$, is the same as that of applying a magnetic field, $\omega_y/\gamma$, in the same direction as the cross axis component of $\vec{\omega}$. Thus, if $\vec{\omega} = \omega_x \hat{X} + \omega_y \hat{Y} + \omega_z \hat{Z}$, the sensed precession frequency, $\Omega$, will be given by

$$\Omega = [(\gamma B + \omega_z)^2 + \omega_x^2 + \omega_y^2]^{1/2}. \tag{3-3}$$

## SIGNAL LOSS DUE TO CROSS AXIS INPUTS

Another effect of a cross axis rotation is to tilt the precession plane such that it is normal to the effective field, $\vec{B}_{eff}$

$$\vec{B}_{eff} = \frac{\omega_x}{\gamma} \hat{X} + \frac{\omega_y}{\gamma} \hat{Y} + (B + \frac{\omega_z}{\gamma}) \hat{Z}. \tag{3-4}$$

The instantaneous normal to the precession plane will always be in the direction of $\vec{B}_{eff}$; however, the manner in which the normal tracks $\vec{B}_{eff}$ depends on how fast $\vec{B}_{eff}$ changes direction and on the inertial conditions of $\vec{M}$ when the change transpires. If $\vec{M}$ initially lies in the plane of precession, this condition can be maintained provided the rate of change of direction of $\vec{B}_{eff}$ is small compared to $|\gamma B_{eff}|$. Violation of this condition will result in $\vec{M}$ tracing out a cone around $\vec{B}_{eff}$. As an example, consider the extreme case where initially $\vec{B}_{eff} = B\hat{Z}$, then as $\vec{M}$ points along the Y-axis, there is an instantaneous change in $\vec{\omega}$ to be $-\omega_y \hat{Y}$. This tilts the effective field toward the $\hat{Y}$ direction. Now $\vec{M}$ maintains a fixed angle with respect to $\vec{B}_{eff}$ and thus moves up out of the horizontal plane (see Figure 3-2). If at some time later, when $\vec{M}$ is at its maximum height, $\vec{\omega}$ goes back to zero, the precession plane will again be a horizontal plane; however, $\vec{M}$ no longer lies in this plane. In fact, if the instantaneous change in $\vec{\omega}$ rotated $\vec{B}_{eff}$ by the angle $\Theta$ , then in the final condition $\vec{M}$ will make an angle $2\Theta$ with the horizontal plane. Recall that the magnetometer senses the horizontal component of $\vec{M}$. *Thus for the example* above the signal has been reduced to have a peak amplitude of $|\vec{M}| \cos 2\Theta$ .

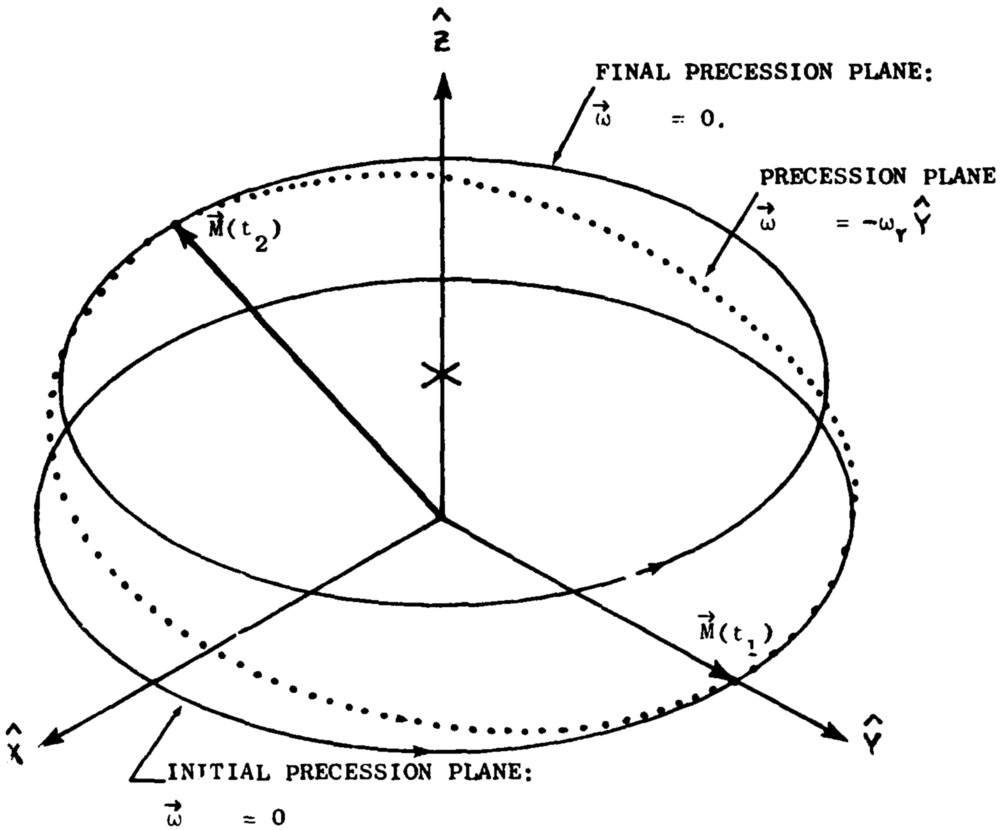


Figure 3-2. Signal Reduction Due to Cross Axis Rate. Initially $\vec{\omega} = 0$, then at $t_1$, $\vec{\omega} = \omega_y \hat{Y}$. This tilts the precession plane. At time $t_2$, $\vec{\omega}$ again becomes zero and the precession plane becomes horizontal. Note now that $\vec{M}$ has a constant $\hat{Z}$ component; and the $\hat{X}$ component has been reduced.

## EFFECT OF OSCILLATORY CROSS-AXIS RATE INPUTS

A problem that has arisen involves oscillatory rates. In particular, if the nuclear gyro experiences an oscillatory rate[13] about a cross axis and at a frequency corresponding to the Larmor frequency, a periodic loss of magnetometer output results. This was demonstrated with a digital simulation of the $^3$He gyro dynamics. The particular case demonstrated was an X-axis gyro in response to an oscillating rate about the Y axis. The cross-axis rate input (Figure 3-3) is described by

$$\omega_y = 0.05\ \gamma B\ \mathrm{sgn}[\cos \gamma Bt] \qquad (3\text{-}5)$$

The resulting path of the magnetization vector, as seen in the gyro frame, is shown to wind its way up the gyro X axis (Figure 3-4). The magnitude of M is unchanged since relaxation effects are ignored, but if the oscillatory input persists, M winds back down into the X-0 plane and then continues its way down the -X axis and back and forth. Since the magnetometer senses the component of M orthogonal to B the effect is to alternately diminish and restore the magnetometer signal. Overall then, the signal-to-noise ratio of the instrument is decreased. In this demonstration time has been scaled in terms of $\gamma B$. For example, if $\gamma B$ is chosen to be $2\pi$ rad/s, then $\omega_y$ has a peak rate of 0.31 rad/s and the total time shown (Figure 3-4) is about 7.5 s. In other words, if the peak input rate is 5% of the Larmor rate, it will take about 7.5 Larmor periods for M to wind its way out of the X=0 plane.

The situation is most easily explained in a rotating frame. For example, approximate $\omega_y$ as

$$\omega_y = 0.05 \, \gamma B \cos \gamma Bt \tag{3-6}$$

Then represent $\omega_y$ as two counter-rotating vectors in the X=0 plane, each of magnitude 0.25 $\gamma B$, starting in the Y-axis direction and rotating at $\gamma B$ rad/s. Then, in the rotating frame, the vector traveling with the rotating frame is stationary, while the other appears to rotate at twice the Larmor rate. The effects of the latter average to zero, but the former causes M to precess about the rotating frame Y axis. In the gyro frame both the Y axis motion and the Larmor precession about the X axis cause the spiral trajectory shown. This situation is a worst-case situation. For oscillatory rates much higher or lower than $\gamma B$, the effect averages to zero.

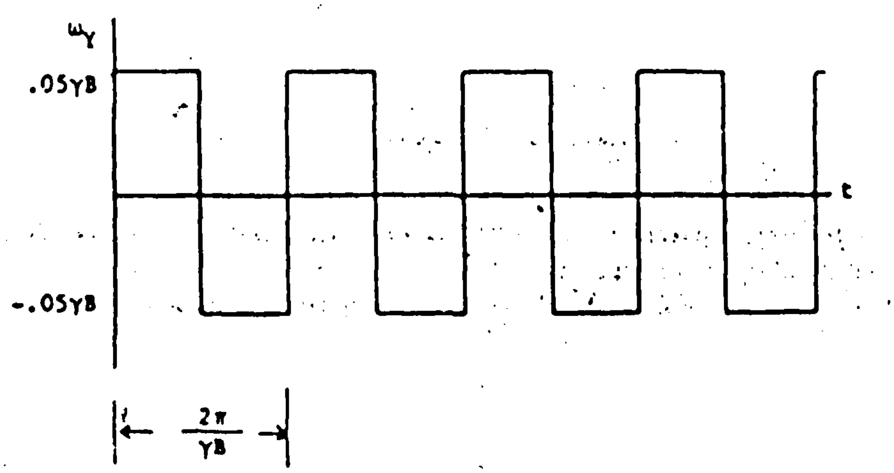


Figure 3-3. Simulated Oscillatory Y-axis Rate.

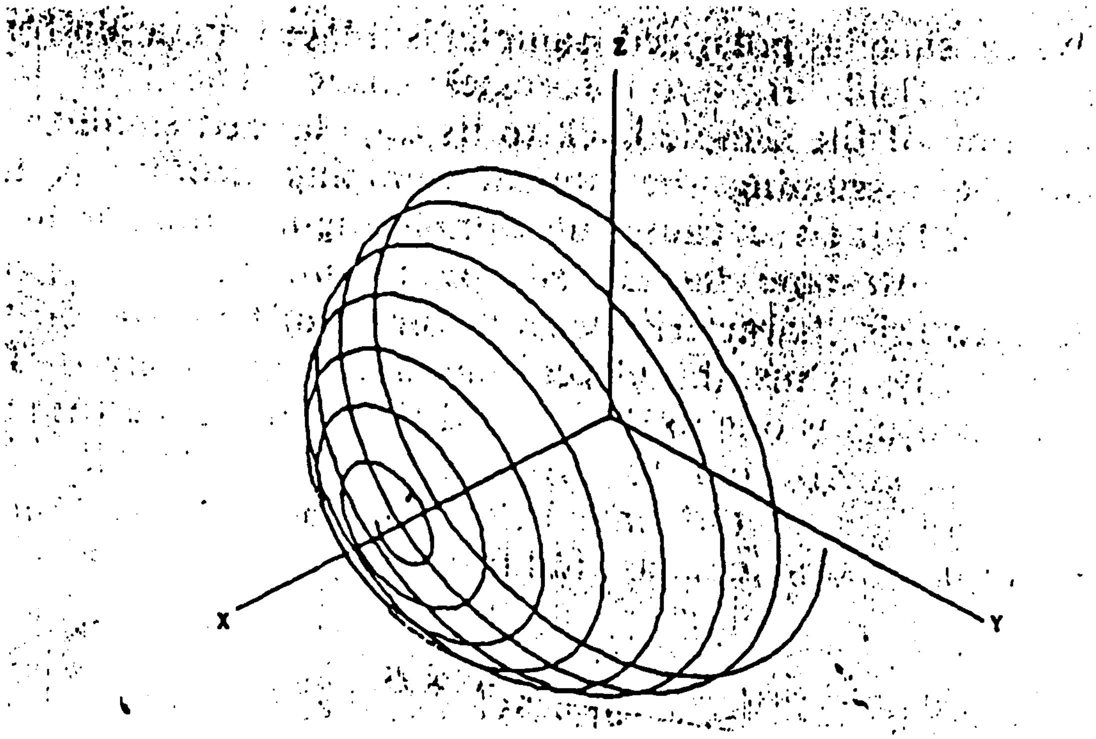


Figure 3-4. Effect on X-axis Gyro of Oscillatory Rate about Y-axis.

## RESOLUTION WITH THREE ORTHOGONAL GYROS

In general, the uncorrected drift, $[\Omega - (\gamma B + \omega_z)]$ is not tolerable. So consider using three identical gyros, rigidly aligned, such that their input axes are orthogonal (Figure 3-5). Then each gyro will undergo the same rotation but, because the input axes are orthogonal, each will be affected differently.

For the case where $\bar{\omega} = \omega_x \hat{X} + \omega_y \hat{Y} + \omega_z \hat{Z}$, the precession frequencies sensed by each gyro are

$$\Omega_x^2 = (\gamma B + \omega_x)^2 + \omega_y^2 + \omega_z^2 \qquad (3\text{-}7a)$$

$$\Omega_y^2 = \omega_x^2 + (\gamma B + \omega_y)^2 + \omega_z^2 \qquad (3\text{-}7b)$$

$$\Omega_z^2 = \omega_x^2 + \omega_y^2 + (\gamma B + \omega_z)^2 \qquad (3\text{-}7c)$$

It is convenient to normalize by dividing both sides of the above by $(\gamma B)^2$, giving:

$$\underline{\Omega}_x^2 = (1 + \underline{\omega}_x)^2 + \underline{\omega}_y^2 + \underline{\omega}_z^2 \qquad (3\text{-}8a)$$

$$\underline{\Omega}_y^2 = \underline{\omega}_x^2 + (1 + \underline{\omega}_y^2) + \underline{\omega}_z^2 \qquad (3\text{-}8b)$$

$$\underline{\Omega}_z^2 = \underline{\omega}_x^2 + \underline{\omega}_y^2 + (1 + \underline{\omega}_z)^2 \qquad (3\text{-}8c)$$

where the underbars indicate normalized quantities.

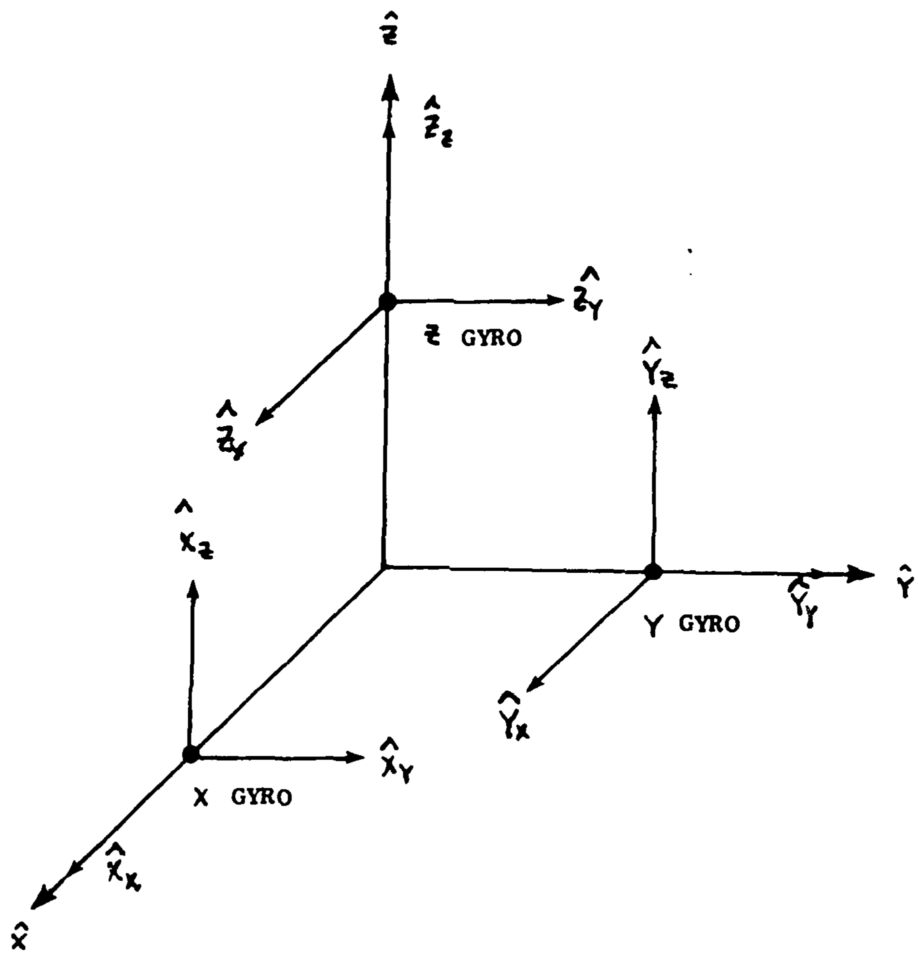


Figure 3-5. Coordinate Frames for Rigid Body Mounting of Three Identical Gyros

Now the question is, do Equations (3-8) uniquely determine $\vec{\omega}$ , and, in general, the answer is no. Knowledge of the time history of $\vec{\omega}$ will not resolve the ambiguity, as the following example will show. Suppose initially $\vec{\omega} = -1/3\ \hat{X} - 1/3\ \hat{Y} - 1/3\ \hat{Z}$. This particular case is resolved unambiguously from (3-8). Furthermore, assume that this condition persists for some time. Then suppose the input changes such that $\vec{\omega} = -0.3333\ \hat{X} - 0.3333\ \hat{Y} - 0.3333\ \hat{Z}$. With only the measurements $\underline{\Omega}_x$, $\underline{\Omega}_y$, $\underline{\Omega}_z$ and knowledge of $\gamma B$, two solutions for $\vec{\omega}$ are possible. One solution is indeed the true solution; the other, however, is $\vec{\omega} = -0.33337\ \hat{X} - 0.33337\ \hat{Y} - 0.33337\ \hat{Z}$. The two solutions are nearly equal, though in opposite directions from the previous known solution. The smaller the step away from $- 1.3\ \hat{X} - 1/3\ \hat{Y} - 1/3\ \hat{Z}$ the closer are the two solutions. Thus it is easy to conceive of the possibility of locking onto the false solution from this starting point.

Let us investigate the source of the ambiguity by considering the space of possible inputs, $\underline{\vec{\omega}}^{b-1}$, $(\underline{\omega}_x, \underline{\omega}_y, \underline{\omega}_z)$, in which we graph Equation (3-8). Figure 3-6 shows the case where $\underline{\vec{\omega}} = 0$. Here the false solution is (-2/3, -2/3, -2/3), and $\underline{\Omega}_x = \underline{\Omega}_y = \underline{\Omega}_z = 1.0$. We see that the information from any one gyro defines a sphere on which the possible values of $\underline{\vec{\omega}}$ lie. The solution(s) then will be the point(s) common to all three spheres. Figure 3-6 is an isometric drawing and so the two solutions plot as the same point; nevertheless one can easily visualize the false solution for this case. Note that for three identical gyros that the centers for the three spheres are located at (-1, 0, 0), (0, -1, 0), and (0, 0, -1) and the corresponding radii are $\underline{\Omega}_x$, $\underline{\Omega}_y$, and $\underline{\Omega}_z$.

To explore this situation further, consider the condition that $\underline{\vec{\omega}}$ lies in the plane defined by the centers of the three spheres. As can be seen from Figure 3-7, there can be no false solution. In this plane the solution is the intersection of three circles. Then, since the three centers are not colinear, there will be at most one point of intersection. And since as one moves out of this plane in either direction, the surfaces of the three spheres will be moving away from one another, there can be no further points of intersection. So the plane of centers defined by (3-12) is the only region where

$$\underline{\omega}_x + \underline{\omega}_y = \underline{\omega}_z = -1 \qquad (3\text{-}9)$$

the solution is unambiguous.

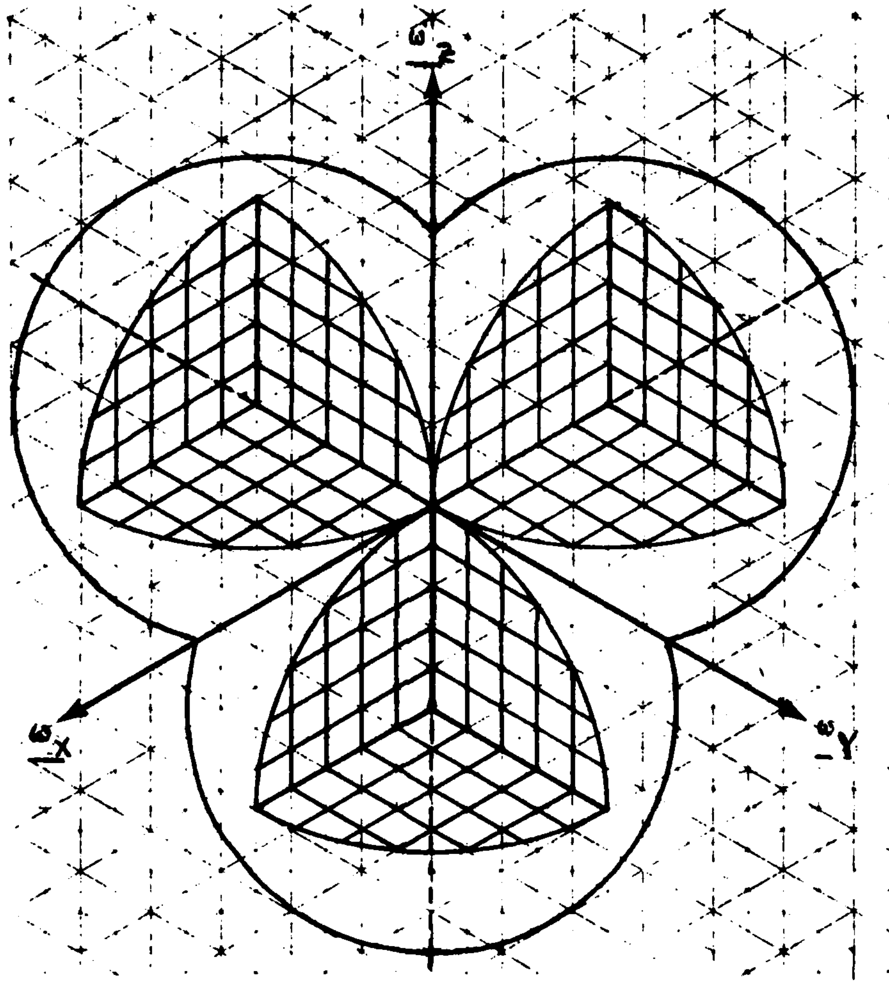


Figure 3-6. Intersecting Spheres Showing Solutions for $\vec{\omega} = 0$. Note the two solutions are (0,0,0) and (-2/3, -2/3, -2/3).

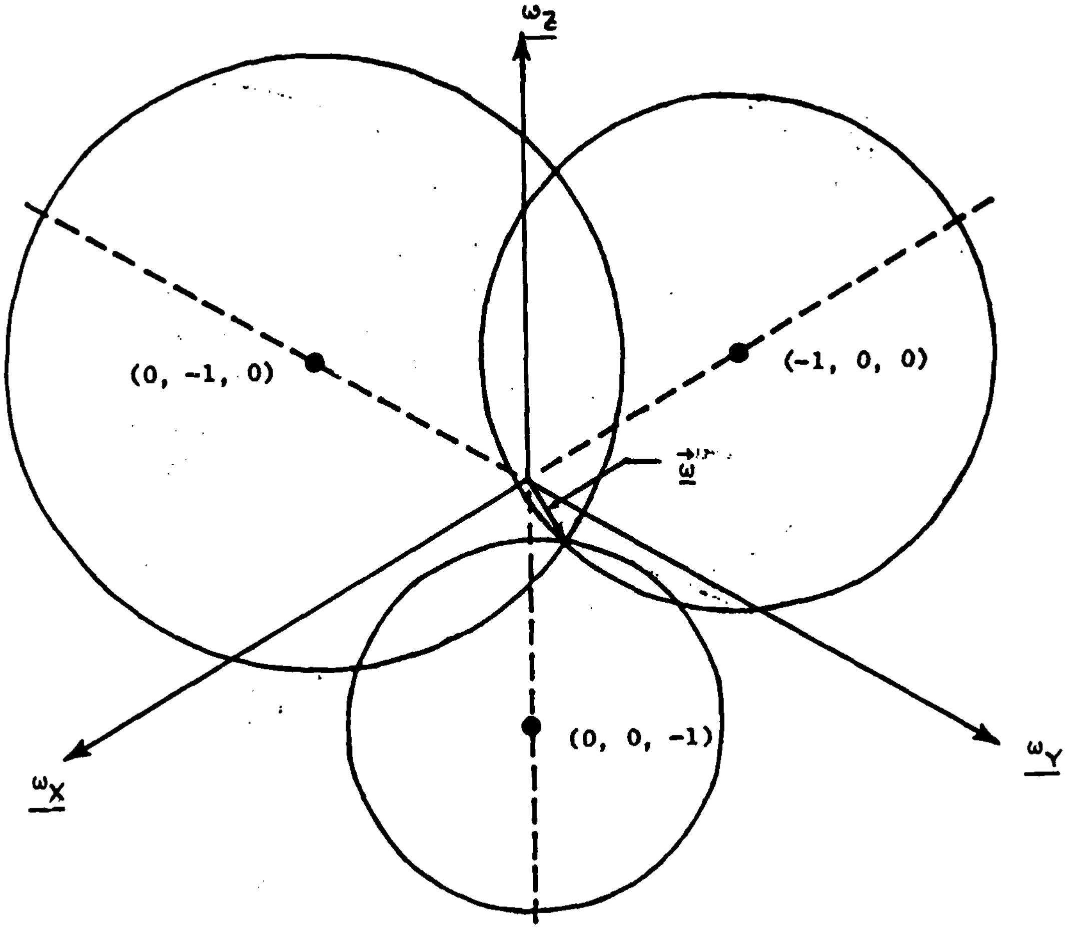


Figure 3-7. Intersecting Circles Showing Unambiguous Case $\vec{\omega} = -2/6\,\hat{X} - 1/6\,\hat{Y} - 3/6\,\hat{Z}$ is in the plane of centers.

What then is the nature of the ambiguity? Consider the case where $\vec{\omega}$ lies outside the plane of centers. Choosing any two of the spheres we see that their intersection must be a circle. Furthermore, the plane of centers cuts this circle in half; i.e., the center of this circle lies in the plane of centers. Now since the third sphere must also pass through $\vec{\omega}$, this sphere will intersect the circle at two points. One is indeed at $\vec{\omega}$ and the second point is the reflection of $\vec{\omega}$ across the plane of centers.

We can now propose a simple criterion for resolving ambiguities. Since one would want to stay away from the resonance condition ($\vec{\omega} = \gamma B$) in general, the Larmor frequency could be chosen such that

$$\omega_x + \omega_y + \omega_z \geq -\gamma B \qquad (3\text{-}10)$$

for all allowable $\vec{\omega}$. Then the proper choice of solutions will always be on the same side of the plane of centers. Another possible criterion, though more restrictive, would be to choose

$$|\gamma B| \geq \sqrt{3}\,|\vec{\omega}|_{max} ; \qquad (3\text{-}11)$$

then the proper solution will be the one with the magnitude less than $1/\sqrt{3}$ ( $|\gamma B|$ ).

## USE OF ADDITIONAL MAGNETIC FIELDS TO NULL CROSS AXIS INPUTS

It is clear from Figure 3-4 that some strategy must be employed to keep the magnetization in the precession plane despite the presence of cross axis rotations. We could consider restricting the operating regime to be always far away from resonance conditions; but there may be yet a more satisfactory approach. Consider again the Bloch equation for an arbitrary $\vec{\omega}$.

$$\frac{d}{dt}\begin{bmatrix} M_x \\ M_y \\ M_z \end{bmatrix} = \begin{bmatrix} 0 & (\gamma B + \omega_z) & -\omega_y \\ -(\gamma B + \omega_z) & 0 & \omega_x \\ \omega_y & -\omega_x & 0 \end{bmatrix}\begin{bmatrix} M_x \\ M_y \\ M_z \end{bmatrix} \qquad (3\text{-}12)$$

If we add coils for generating magnetic fields in the $\hat{X}$ and $\hat{Y}$ axes we get

$$\frac{d}{dt}\begin{bmatrix} M_x \\ M_y \\ M_z \end{bmatrix} = \begin{bmatrix} 0 & (\gamma B + \omega_z) & -(\gamma B_y+\omega_y) \\ -(\gamma B + \omega_z) & 0 & (\gamma B_x+\omega_x) \\ (\gamma B_y+\omega_y) & -(\gamma B_x+\omega_x) & 0 \end{bmatrix}\begin{bmatrix} M_x \\ M_y \\ M_z \end{bmatrix} \qquad (3\text{-}13)$$

Thus if we can provide two control loops to keep both ( $B_x + \omega_x$) and ($\gamma B_x + \omega_y$) zero, we can remove the effects of cross axis inputs.

## THE THREE DEGREE-OF-FREEDOM GYRO

Since the nuclear gyro is sensitive to cross axis inputs, it is theoretically possible to determine all three components of $\vec{\omega}$ with a single device. To do this three magnetometers are required, one to measure each components of $\vec{M}$. The procedure for determining $\vec{\omega}$ from measurements of the components of $\vec{M}$ is as follows:

1) Take three consecutive readings of $\vec{M}$, $\vec{M}_a$, $\vec{M}_b$, and $\vec{M}_c$.

2) Form the vectors $\vec{M}_A = \vec{M}_b - \vec{M}_a$ and $\vec{M}_B = \vec{M}_c - \vec{M}_b$.

3) Assuming $\vec{\omega}$ is constant during the three readings, then the vectors $\vec{M}_A$ and $\vec{M}_B$ lie in the precession plane and $\vec{M}_A \times \vec{M}_B / |\vec{M}_A| |\vec{M}_B|$ is a unit vector in the direction $-(\gamma B_x + \omega_x) \hat{X} - (\gamma B_y + \omega_y) \hat{Y} - (\gamma B + \omega_z) \hat{Z}$ which is denoted as $\hat{n}$.

4) Next choose any of the three measurements, say $\vec{M}_b$, and determine $\vec{M}_b \times \hat{n} = |\vec{M}_b| \sin \phi$ or

$$\sin \phi = \frac{\vec{M}_b \times \hat{n}}{|\vec{M}_b|} \tag{3-14}$$

5) The radius of the precession plane is given by $|\vec{M}_b| \sin \phi = |\vec{M}_b \times \hat{n}|$.

6) Now $|\vec{\omega}|$ can be determined (see Figure 3-8), from the radius of the precession plane, the time between measurements, and the measurements $\vec{M}_a$ and $\vec{M}_b$.

$$\alpha = \cos^{-1} \frac{2|\vec{M}_b \times \hat{n}|^2 - |\vec{M}_c - \vec{M}_a|}{2|\vec{M}_b \times \hat{n}|^2}$$

$$|\vec{\omega}' \quad | = \alpha/\Delta t$$

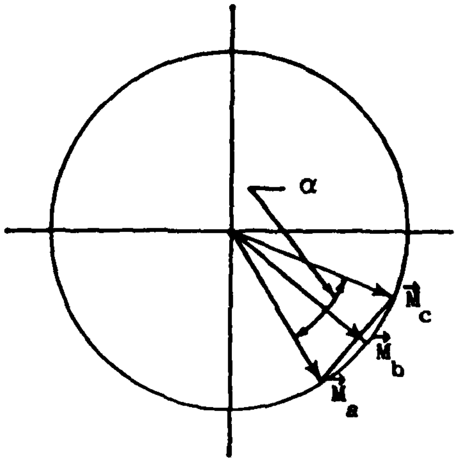


Figure 3-8. Determination of $\vec{\omega}$ from three measurements of $\vec{M}$. The veiw is directly into the precession plane. Note $\Delta t$ is the time between measurements $\vec{M}_c$ and $\vec{M}_a$.

Assuming perfect measurements and no noise this scheme works very well. Figure 3-9 shows two $\vec{M}$ trajectories for a situation where a step change in $\vec{\omega}$ occurs. In this case the size of the step is 10% of the Larmor frequency and is applied along the $\hat{Y}$ axis at the time when $\vec{M} = |\vec{M}| \hat{Y}$. As can be seen, the precession plane tips down $\sim$ 5.7 deg (0.01 rad) with no control; but is visually unaffected when a magnetic field is applied to buck out the rotation. With control applied, the vertical component of the magnetization reaches only a value of $-3.11 \times 10^{-8}$ $|\vec{M}(0)|$ , and at a sample rate of 50 samples per Larmor period, the cross axis input is nulled after only three samples.

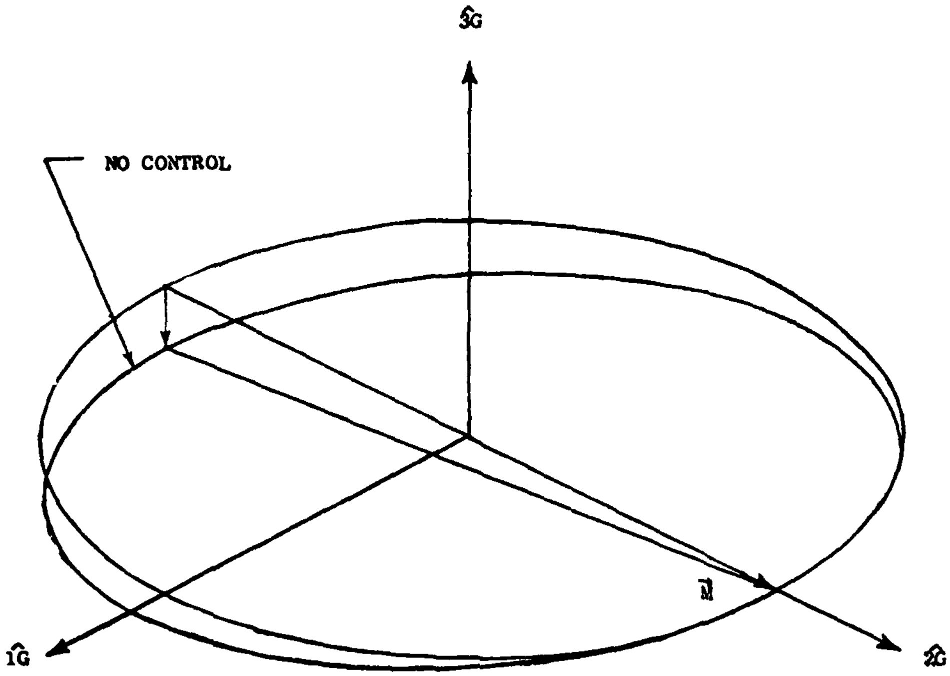


Figure 3-9. Removal of Cross Axis Effect with 3 DOF Gyro Scheme The horizontal precession plane is the plane for zero cross axis rate, the tilted precession plane is that for $\omega_y = 0.1\ \gamma B\ \hat{Y}$. Use of 3 DOF gyro control scheme removes $\omega_y$ effects leaving the initial horizontal precession plane virtually unchanged.

There are some problems with this approach. One is that the computation involved will limit the sample rate; but probably more crucial is the susceptibility to noise. Figure 3-10 shows the source of the noise sensitivity. Here the first and third measurements are exact but the second is noisy. Since the algorithm to determine $\vec{\omega}$ fits a circular precession plane to these three points, we see that the same amount of noise causes more problems for fast sample rates than for slow. So the measurement noise also places restrictions on the sample rate.

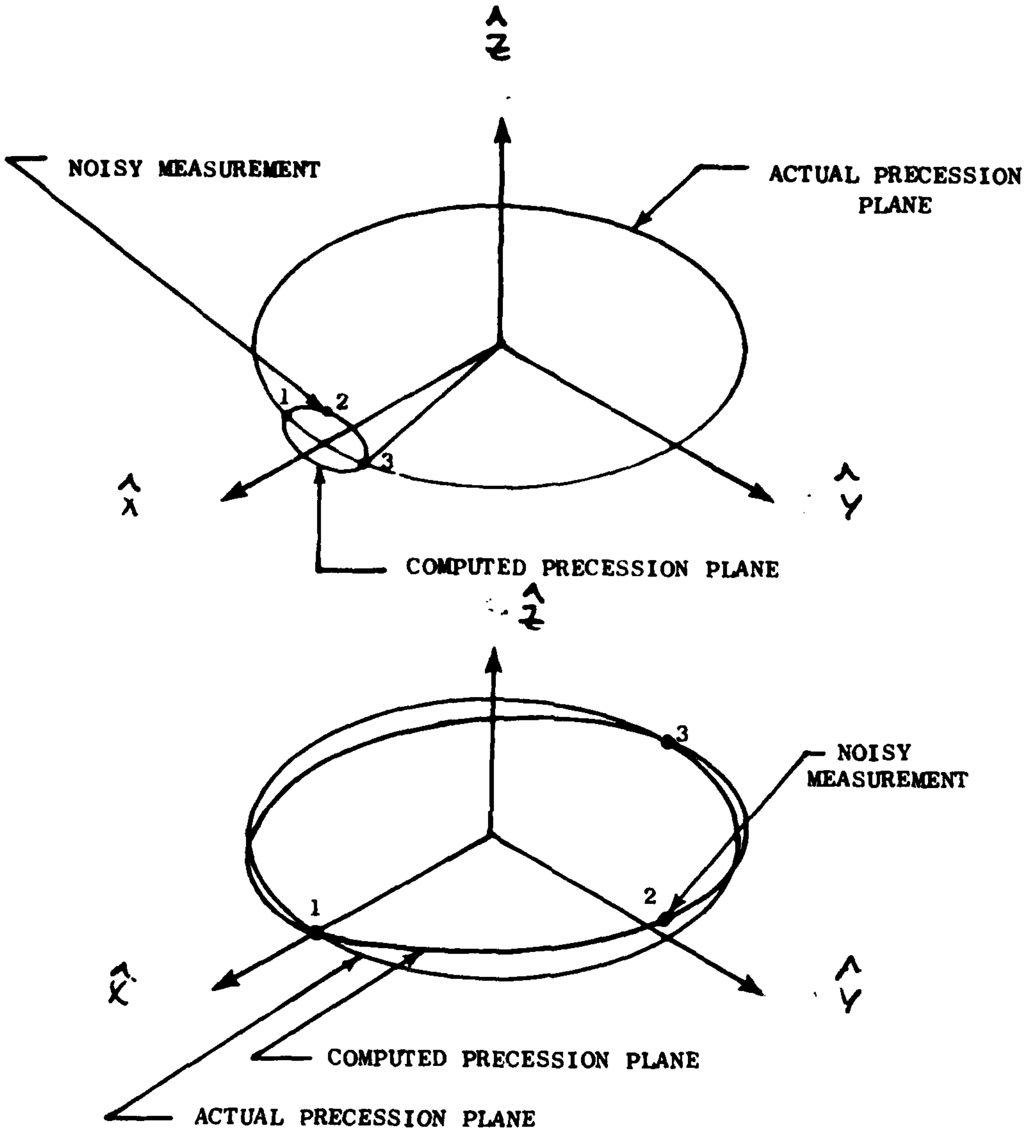


Figure 3-10. Effect of Measurement Noise of 3 DOF Gyro Scheme
The upper sketch shows the effdct of a noisy measurement for a sample rate with respect to precession rate. The computed precession plane is orthogonal to the actual precession plane. The lower sketch shows :he effect of the same amount of noise when the sample rate is slow. Here the actual and computed precession planes are nearly the same.

One final problem with this scheme should also be mentioned; and that is the effect of magnetometer drift on stability of the applied field. Since the SQUID magnetometers require a small, but finite current in the pickup coil, they will also generate magnetic fields. The effects of the pickup coil currents, transverse to the main field coil, will be small; but the pickup coil current in the same axis will add to the applied field directly. If this current were constant, its effect could be modeled out; however, a current change of $1 \times 10^{-9}$ amps gives a drift of $\sim 5 \times 10^{-5}$ rad/sec for a typical device.

## THREE ORTHOGONAL SINGLE DEGREE-OF-FREEDOM (SDOF) GYROS

We now return to see what we can do with three orthogonal SDOF gyros, each having one or two magnetometers orthogonal to each other (if two) and to the applied field axis. Since we now have added field coils in the cross axes to null cross axis rates, this is not the same problem as was previously investigated. These added field coils take out different components of the body rate for each of the three gyros. So while the solution for $\vec{\omega}$ is still the intersection of three spheres the centers of the three spheres are no longer fixed. Just as the applied field moves the center of a given sphere along the negative input axis for that particular gyro, so too do the feedback fields move the center along the cross axes.

The question of ambiguities is not as clear here as it was for the case with no cross-axis field coils. However, one simple algorithm appears to work very well for determining $\vec{\omega}$ from the three gyros.

The procedures is as follows:

1) Measure the precession frequency for each gyro.

2) Compar. .is measured frequency with the zero input Larmor frequency and take the difference to be the rate about the input axis.

3) Use these estimated rates to determine the required cross axis fields.

4) Continue this procedure.

Figure 3-11 shows the response to a step in $\vec{\omega}$. The step size is 25% of the Larmor frequency and is applied along the $\hat{z}$ axis. The significance to the time scale on Figure 3-11 is that the precession frequency of each gyro is assumed to be determined in one time unit. So let us look at what is involved in determining the precession frequency from the SQUID magnetometer(s) output. If one assumes that, during the measurement period, the precession frequency is constant and the gyro housing rotation rates are small compared to the Larmor frequency, then the SQUID output will be a sinusoidal signal, within a certain band, centered at the Larmor frequency. If the unwanted low- and high-frequency bands are filtered out then the SQUID output $M_s(t)$ will have the form

$$M_s(t) = A \sin \omega t + B \cos \omega t. \tag{3-15}$$

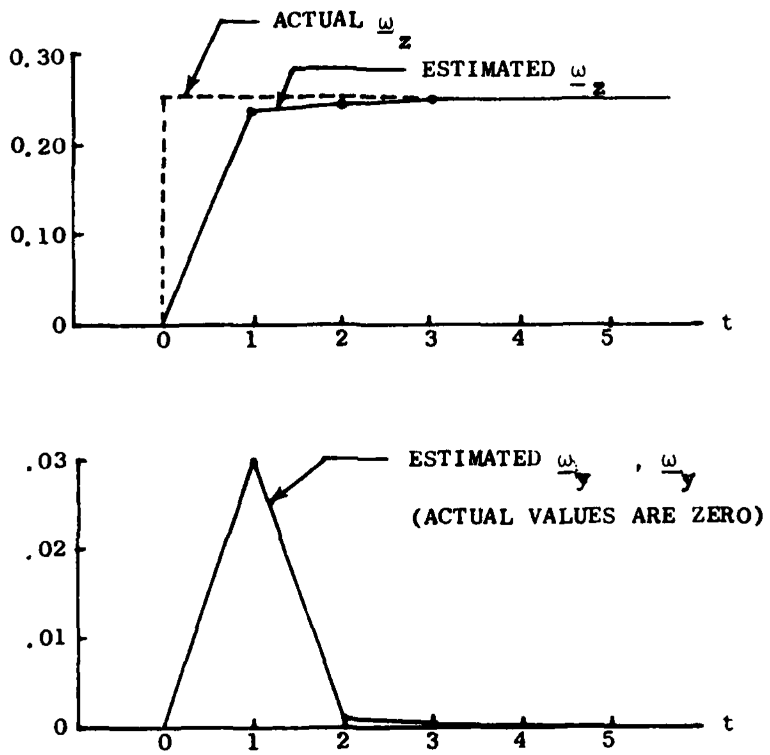


$$\vec{\underline{\omega}} = \begin{cases} 0 & \text{for } t < 0 \\ 0.25\ \hat{z} & \text{for } t \geq 0 \end{cases}$$

Figure 3-11. Response to a Step in $\vec{\underline{\omega}}$.
Note one unit of time is the time required to measure the precession frequencies in all three gyros.

Consider sampling this signal at a fixed sample period, T sec. Then it is shown that the nth sample is given by

$$
\begin{aligned}
M_s(n) &= B\delta(T) + (A \sin \omega T - B \cos \omega T)\ \delta(T-1) \\
&\quad + 2 \cos \omega T\ M_s(n-1) - M_s(n-2).
\end{aligned}
\tag{3-16}
$$

We can write this out in matrix form as

$$
\begin{bmatrix} M_s(0) \\ M_s(1) \\ M_s(2) \\ M_s(3) \\ M_s(4) \\ \vdots \end{bmatrix}
=
\begin{bmatrix}
1 & 0 & 0 & 0 \\
0 & 1 & M_s(0) & 0 \\
0 & 0 & M_s(1) & M_s(0) \\
0 & 0 & M_s(2) & M_s(1) \\
0 & 0 & M_s(3) & M_s(2) \\
\vdots & \vdots & \vdots & \vdots
\end{bmatrix}
\begin{bmatrix} B \\ A \sin \omega T - B \cos \omega T \\ 2 \cos \omega T \\ -1 \end{bmatrix}
\tag{3-17}
$$

The upper left partition is due to initial conditions so if we wait two sample periods we have

$$\underbrace{\begin{bmatrix} M_s(2) \\ M_s(3) \\ M_s(4) \\ \cdot \\ \cdot \\ \cdot \end{bmatrix}}_{y} = \underbrace{\begin{bmatrix} M_s(1) & M_s(0) \\ M_s(2) & M_s(1) \\ M_s(3) & M_s(2) \\ \cdot & \cdot \\ \cdot & \cdot \\ \cdot & \cdot \end{bmatrix}}_{p} \underbrace{\begin{bmatrix} 2\cos \omega T \\ -1 \end{bmatrix}}_{a} \qquad (3\text{-}18)$$

Now define $2 \cos \omega T = a_1$ and $-1 = a_2$ and consider the case where we have noise $\gamma$ such that

$$y = pa + \gamma \qquad (3\text{-}19)$$

We know, via measurements, both y and A; and we can get a best least squares estimate of a as

$$\hat{a} = (p^T p)^{-1} p^T y \qquad (3\text{-}20)$$

Since we know $a_2 = -1$ we could consider the convergence of $\hat{a}_2$ to -1 as a simple test for a good estimate of $a_1$. Finally, we estimate the precession frequency from $\hat{a}_1$ as

$$\hat{\omega} = \frac{1}{T} \cos^{-1} \left(\frac{\hat{a}_1}{2}\right) \qquad (3\text{-}21)$$

Then the estimates of $\omega$, one for each gyro, can be used to determine the fields necessary to cancel the cross axis rates. Note that if fields are generated, there will be changes in the precession frequencies of the three gyros. Thus the next two samples will again exhibit the transient terms in Equation (3-17).

## 4.0 A PRACTICAL IMPLEMENTATION

The previous chapter investigated the dynamics of the $^3$He gyro and pointed out several problems due to cross axis sensitivities. The latter portion however hinted that these effects could perhaps be removed with a 3-orthogonal gyro configuration. Clearly this implementation would work with the gyros mounted on a stable platform. This, however, would defeat the purpose of developing a no-moving parts technology and would be difficult to implement in an all cryogenic inertial measurement unit. The use of additional applied fields to null out cross axis rates is the equivalent of a stable platform approach and requires no moving parts.

The basic strategy then is to measure the magnetization in each gyro and from these measurements estimate each of the Larmor precession frequencies. So the first task is to implement an estimator based on a measurement from a SQUID sensing one component of $\vec{M}$. The most general expression for the component of magnetization sensed by the SQUID is

$$M_s(t) = A \sin \omega t + B \cos \omega t + C \qquad (4\text{-}1)$$

Taking the Z-transform yields

$$M_s(z) = A\,\frac{\sin\ \omega T_Z^{-1}}{1-(2\cos\ \omega T)Z^{-1}+Z^{+2}} + B\,\frac{1(\cos\ \omega\ T)Z^{-1}}{1-(2\cos\ \omega\ T)Z^{-1}+Z^{+2}} + C\,\frac{1}{1-Z^{-1}} \qquad (4\text{-}2)$$

Then from Equation (4-2) the nth sample is given by

$$\begin{aligned} M_s(n) = {} & (B+C)\,\delta(T) + (A\sin\omega T-(2C+B)\cos\omega T-B)\,\delta(T-1) \\ & + (C+B\cos\omega T-A\sin\omega T)\ \delta(T-2) \\ & + (2\cos\ \omega T+1)\ M_s(n-1) - (2\cos\omega T+1)M_s(n-2)+M_s(n-3) \qquad (4\text{-}3) \end{aligned}$$

In matrix form this becomes

$$\begin{bmatrix} M_s(0) \\ M_s(1) \\ M_s(2) \\ \hdashline M_s(3) \\ M_s(4) \\ M_s(5) \\ M_s(6) \\ \vdots \\ M_s(n) \end{bmatrix} = \left[\begin{array}{ccc:ccc} 1 & 0 & 0 & 0 & 0 & 0 \\ 0 & 1 & 0 & M_s(0) & 0 & 0 \\ 0 & 0 & 1 & M_s(1) & M_s(0) & 0 \\ \hdashline & & & M_s(2) & M_s(1) & M_s(0) \\ & & & M_s(3) & M_s(2) & M_s(1) \\ & & & M_s(4) & M_s(3) & M_s(2) \\ & & & M_s(5) & M_s(4) & M_s(3) \\ & & & \vdots & \vdots & \vdots \\ & & & M_s(n-1) & M_s(n-2) & M_s(n-3) \end{array}\right] \left[\begin{array}{c} B+C \\ A\ \sin\omega T - (2C+B)\cos\ \omega T + B \\ C + B\cos\ \omega T - A\sin\omega\ T \\ \hdashline 2\cos\ \omega T + 1 \\ -\ (2\cos\ \ T + 1) \\ 1 \\ \\ \\ \\ \end{array}\right] \qquad (4\text{-}4)$$

Finally removing the transient terms gives

$$\underbrace{\begin{bmatrix} M_s(3) \\ M_s(4) \\ M_s(5) \\ M_s(6) \\ \vdots \\ M_s(n) \end{bmatrix}}_{y} = \underbrace{\begin{bmatrix} M_s(2) & M_s(1) & M_s(0) \\ M_s(3) & M_s(2) & M_s(1) \\ M_s(4) & M_s(3) & M_s(2) \\ M_s(5) & M_s(4) & M_s(3) \\ \vdots & \vdots & \vdots \\ M_s(n-1) & M_s(n-2) & M_s(n-3 \end{bmatrix}}_{P} \underbrace{\begin{bmatrix} 2\cos\ T+1 \\ -(2\cos\ T+1) \\ 1 \end{bmatrix}}_{a} \tag{4-5}$$

Note that the addition of the steady state term to $M_s(t)$ adds another parameter to estimate and correspondingly adds another column to the P matrix. Again though the best least squares estimate of a is

$$\hat{a} = (P^T P)^{-1} P^T y \tag{4-6}$$

Now $\hat{a}_3$ should converge to 1 and either $\hat{a}_1$ or $\hat{a}_2$ can be used to estimate $\omega$.

A program, written in BASIC, is included in the appendix which performs this estimation. The program simulates the dynamics of 3-orthogonal $^3$He gyros via theoretically derived state transition matrices to describe the motion of the magnetization vector. From this the SQUID measurements are determined and finally $\hat{a}$ is computed. For reasons not yet understood the two parameter estimator Equation (3-10) was sometimes superior to the three parameter estimator Equation (4-6). Thus both estimators are exercised and convergence criteria for each evaluated to choose the better estimate of $\omega$.

The approach appears to offer some promise for accomplishing the estimation of $\omega$ with more than adequate bandwidth for most applications requiring precision gyros. The remainder of the effort would be to use $\hat{\omega}$ to generate the cross axis fields in each gyro to remove cross coupling terms. An optimum control law would have to be developed to accomplish to this task. This work was not completed due to termination of the project.

## 5.0 CONCLUSIONS AND RECOMMENDATIONS

The problems inherent with rotation sensing via observation of free precession of a nuclear species seem largely solvable by mounting the devices on a stable platform. Since the equivalent of a stable platform can be accomplished by generating cross axis magnetic fields it is a promising technology for high precision rotation measurement with no moving parts. The $^3He$ device, in particular, promises high resolution and used in conjunction with other cryogenic instruments (i.e., accelerometers, gravity gradiometers, computers, and clocks) could provide an all cryogenic inertial measurement unit for very demanding applications.[14]

There is a fair amount of work to be finished before the promise becomes a reality however. From this end additional effort is required to optimize the estimation scheme and then to develop and optimize the control law.

From the hardware point, the Stanford device should be assembled and tested to verify the expected sensitivity. Finally, a test of the overall scheme should be performed, substituting the Stanford device, with actual measurements, for one of the simulated devices.

## REFERENCES


1. Kanegsberg, E., Volk, C.H., Mark, J.G., Williams, H.E., "Investigation of Bias Stability and Cross Axis Effects and Brassboard Gyro Conceptual Design for a Nuclear Magnetic Resonance Gyro," Air Force Avionics Laboratory, AFAL-TR-79-1155, Oct 1979.

2. Simpson, J.H., Tarasevich, M., Ferriss, L.S., "Nuclear Magnetic Resonance Gyro Design and Test Study," Air Force Avionics Laboratory, AFAL-TR-79-1199, Dec 1979.

3. Britting, K.R., Madden, S.J., Hildebrant, R.A., "Assessment of the Impact of Gradiometer Techniques on the Performance of Inertial Navigation Systems," Air Force Cambridge Research Laboratories, AFCRL-71-0465, Sep 1971.

4. Colegrove, F.D., Schearer, L.D., Walters, G.K., Phys. Rev. 132, 2561 (1963).

5. Taber, M.A., "Spin-Lattice Relaxation of Dilute Solutions of Polarized $He^3$ in Liquid $He^4$ in Low Magnetic Fields at 4K," PhD Thesis, Stanford University, Department of Physics, 1978.

6. Cabrera, B., "The use of Superconducting Shields for Generating Ultra-Low Magnetic Field Regions and Several Related Experiments," PhD Thesis, Stanford University, Department of Physics, 1975.

7. Giffard, R.P., J. of Low Temp. Phys., Vol. 6, pp. 533, 1972.

8. SHE Manufacturer Handbook, SHE Corporation, San Diego, CA, 92121.

9. Silver, A.H., Zimmerman, J.E., Phys. Rev., Vol. 157, pp. 317, May 1967.

10. Zimmerman, J.E., et. al., J. of Applied Phys., Vol. 41, No. 4, pp. 1572-1580, March 1970.

11. Shaw, G.L., "Cross Axis Sensitivity in a Nuclear Gyroscope," Proceedings of the Science and Engineering Symposium, Dayton, OH, Oct 1981.

12. Abragam, A., The Principles of Nuclear Magnetism, Oxford Press, 1973.

13. Shaw, G.L., "Sensitivity to Cross Axis Oscillations in a Single-Axis Nuclear Gyroscope," AIAA Journal of Guidance, Control and Dynamics, Vol. 7, No. 4, pp 501, Jul-Aug 1984.

14. Shaw, G.L., Taber, M.A., "The $^3He$ Gyro for an all Cryogenic Inertial Measurement Unit," Proceedings of the Symposium Gyro Technology 1983, Stuttgart, Germany, Sept 1983.

# APPENDIX

Program listings for $^3He$ gyro 3-axis dynamic simulation and Larmor frequency estimation

```
01234567890123456789     ** RSX-11M V3.2 **     [113,1]HELIUM - NO PAGE LIMIT
01234567890123456789     ** RSX-11M V3.2 **     FORM #0 - NORMAL HARDWARE FORM
01234567890123456789     ** RSX-11M V3.2 **     NO IMPLIED FORM FEED
01234567890123456789     ** RSX-11M V3.2 **     DPO:[113,1]HELIUM.BAS;12
```

```
  [[[[[[        11          11          333333                    11
  [[[[[[        11          11          333333                    11
  [[          1111        1111        33      33                1111
  [[          1111        1111        33      33                1111
  [[            11          11                33                  11
  [[            11          11                33                  11
  [[            11          11              33        ,,,,        11
  [[            11          11              33        ,,,,        11
  [[            11          11                33      ,,,,        11
  [[            11          11                33      ,,,,        11
  [[            11          11        33      33        ,,        11
  [[            11          11        33      33        ,,        11
  [[[[[[      111111      111111        333333        ,,        111111
  [[[[[[      111111      111111        333333        ,,        111111
```

```
HH      HH  EEEEEEEEEE  LL              IIIIII    UU      UU  MM      MM
HH      HH  EEEEEEEEEE  LL              IIIIII    UU      UU  MM      MM
HH      HH  EE          LL                II      UU      UU  MMMM  MMMM
HH      HH  EE          LL                II      UU      UU  MMMM  MMMM
HH      HH  EE          LL                II      UU      UU  MM  MM  MM
HH      HH  EE          LL                II      UU      UU  MM  MM  MM
HHHHHHHHHH  EEEEEEEE    LL                II      UU      UU  MM      MM
HHHHHHHHHH  EEEEEEEE    LL                II      UU      UU  MM      MM
HH      HH  EE          LL                II      UU      UU  MM      MM
HH      HH  EE          LL                II      UU      UU  MM      MM
HH      HH  EE          LL                II      UU      UU  MM      MM
HH      HH  EE          LL                II      UU      UU  MM      MM
HH      HH  EEEEEEEEEE  LLLLLLLLLL      IIIIII    UUUUUUUUUU  MM      MM
HH      HH  EEEEEEEEEE  LLLLLLLLLL      IIIIII    UUUUUUUUUU  MM      MM
```


```
01234567890123456789     ** RSX-11M V3.2 **     [113,1]HELIUM - NO PAGE LIMIT
01234567890123456789     ** RSX-11M V3.2 **     FORM #0 - NORMAL HARDWARE FORM
01234567890123456789     ** RSX-11M V3.2 **     NO IMPLIED FORM FEED
01234567890123456789     ** RSX-11M V3.2 **     DPO:[113,1]HELIUM.BAS;12
```

```
10 DIM A(3),P(50,3),V(3,3),O(3),T(3,3),Y(50),U(3,3)
11 DIM Z(3,3),W(3),M(3,3),G(3,3),C(3,3),N(3,3)
12 DIM O(53,3)
30 FOR I=1 TO 3
31 FOR J=1 TO 3
32 LET G(I,J)=0
33 NEXT J
34 NEXT I
40 PRINT "ENTER THE NUMBER CF ROWS FOR THE P MATRIX"
41 INPUT N
42 LET M=3
50 PRINT "ENTER THE LARMOR FREQUENCIES FOR THE X,Y,AND Z GYROS"
51 INPUT G(1,1)
52 INPUT G(2,2)
53 INPUT G(3,3)
54 PRINT "ENTER M(0) FOR THE X GYRO X,Y,Z COMPONENTS"
55 INPUT M(1,1)
56 INPUT M(2,1)
57 INPUT M(3,1)
58 PRINT "ENTER M(0) FOR THE Y GYRO X,Y,Z COMPONENTS"
59 INPUT M(1,2)
60 INPUT M(2,2)
61 INPUT M(3,2)
62 PRINT "ENTER M(0) FOR THE Z GYRO X,Y,Z COMPONENTS"
63 INPUT M(1,3)
64 INPUT M(2,3)
65 INPUT M(3,3)
66 PRINT " ENTER THE TIME STEP"
67 INPUT T
70 PRINT "ENTER THE ROTATION RATE X,Y,Z COMPONENTS"
71 INPUT W(1)
72 INPUT W(2)
73 INPUT W(3)
97 REM ######################################################################
98 FOR J=1 TO (N+3)
99 REM ***************  X GYRC  ***************
100 LET C(1,3)=G(1,1)+W(1)
101 LET C(2,3)=G(2,1)+W(2)
102 LET C(3,3)=G(3,1)+W(3)
110 GOSUB 500
120 LET N(1,1)=Z(1,1)*M(1,1)+Z(1,2)*M(2,1)+Z(1,3)*M(3,1)
121 LET N(2,1)=Z(2,1)*M(1,1)+Z(2,2)*M(2,1)+Z(2,3)*M(3,1)
122 LET N(3,1)=Z(3,1)*M(1,1)+Z(3,2)*M(2,1)+Z(3,3)*M(3,1)
125 LET M(1,1)=N(1,1)
126 LET M(2,1)=N(2,1)
127 LET M(3,1)=N(3,1)
140 REM ***************  Y GYRC  ***************
141 LET C(1,3)=G(1,2)+W(1)
142 LET C(2,3)=G(2,2)+W(2)
143 LET C(3,3)=G(3,2)+W(3)
145 GOSUB 500
150 LET N(1,2)=Z(1,1)*M(1,2)+Z(1,2)*M(2,2)+Z(1,3)*M(3,2)
151 LET N(2,2)=Z(2,1)*M(1,2)+Z(2,2)*M(2,2)+Z(2,3)*M(3,2)
152 LET N(3,2)=Z(3,1)*M(1,2)+Z(3,2)*M(2,2)+Z(3,3)*M(3,2)
155 LET M(1,2)=N(1,2)
156 LET M(2,2)=N(2,2)
157 LET M(3,2)=N(3,2)
180 REM **************  Z GYRC  ***************
181 LET C(1,3)=G(1,3)+W(1)
182 LET C(2,3)=G(2,3)+W(2)
183 LET C(3,3)=G(3,3)+W(3)
185 GOSUB 500
190 LET N(1,3)=Z(1,1)*M(1,3)+Z(1,2)*M(2,3)+Z(1,3)*M(3,3)
191 LET N(2,3)=Z(2,1)*M(1,3)+Z(2,2)*M(2,3)+Z(2,3)*M(3,3)
```

```
192 LET N(3,3)=Z(3,1)*M(1,3)+Z(3,2)*M(2,3)+Z(3,3)*M(3,3)
195 LET M(1,3)=N(1,3)
196 LET M(2,3)=N(2,3)
197 LET M(3,3)=N(3,3)
200 LET Q(J,1)=M(2,1)
201 LET Q(J,2)=M(3,2)
202 LET Q(J,3)=M(1,3)
205 NEXT J
210 REM *****************************************************************
250 REM ****** NOW READY TO ESTIMATE THE LARMOR FREQUENCIES ******
251 REM
252 REM
255 REM ***************  X GYRO  ***************
256 REM
260 FOR J=1 TO N
261 LET Y(J)=Q((J+3),1)
262 LET P(J,1)=Q((J+2),1)
263 LET P(J,2)=Q((J+1),1)
264 LET P(J,3)=Q(J,1)
270 NEXT J
275 GOSUB 987
280 GOSUB 910
285 GOSUB 971
290 GOSUB 890
295 PRINT A(1),A(2),A(3),D
296 GOSUB 650
297 IF M=3 GO TO 350
298 GOSUB 2000
350 REM ***************  Y GYRO  ***************
360 FOR J=1 TO N
361 LET Y(J)=Q((J+3),2)
362 LET P(J,1)=Q((J+2),2)
363 LET P(J,2)=Q((J+1),2)
364 LET P(J,3)=Q(J,2)
370 NEXT J
375 GOSUB 987
380 GOSUB 910
385 GOSUB 971
390 GOSUB 890
395 PRINT A(1),A(2),A(3),D
396 GOSUB 650
397 IF M=3 GO TO 450
398 GOSUB 3000
450 REM ***************  Z GYRO  ***************
460 FOR J=1 TO N
461 LET Y(J)=Q((J+3),3)
462 LET P(J,1)=Q((J+2),3)
463 LET P(J,2)=Q((J+1),3)
464 LET P(J,3)=Q(J,3)
470 NEXT J
475 GOSUB 987
480 GOSUB 910
485 GOSUB 971
490 GOSUB 890
492 PRINT A(1),A(2),A(3),D
493 GOSUB 650
495 IF M=3 GO TO 605
496 GOSUB 4000
497 GO TO 605
605 INPUT X
606 IF X=0 GO TO 70
610 GO TO 9999
640 REM *****************************************************************
641 REM * THIS SUBROUTINE TESTS TO SEE IF THE TWO OR THE THREE           *
642 REM *  PARAMETER ESTIMATOR WORKS BETTER                              *
643 REM *****************************************************************
```

```
650 IF ABS(D)<1.00000E-05 GO TO 655
651 IF ABS(A(2)+A(1))>.1 GO TO 655
652 IF ABS(A(3)-1)>.1 GO TO 655
653 LET M=3
654 GO TO 660
655 LET M=2
660 RETURN
2000 REM ***************  X GYRO  ***************
2001 REM                           2PE
2002 FOR J=1 TO N
2003 LET Y(J)=Q((J+2),1)
2004 LET P(J,1)=Q((J+1),1)
2005 LET P(J,2)=Q(J,1)
2010 NEXT J
2015 GOSUB 987
2020 GOSUB 1000
2025 GOSUB 971
2030 GOSUB 890
2035 PRINT A(1),A(2)
2040 LET M=3
2045 RETURN
3000 REM ***************  Y GYRO  ***************
3001 REM                           2PE
3002 FOR J=1 TO N
3003 LET Y(J)=Q((J+2),2)
3004 LET P(J,1)=Q((J+1),2)
3005 LET P(J,2)=Q(J,2)
3010 NEXT J
3015 GOSUB 987
3020 GOSUB 1000
3025 GOSUB 971
3030 GOSUB 890
3035 PRINT A(1),A(2)
3040 LET M=3
3045 RETURN
4000 REM ***************  Z GYRO  ***************
4001 REM                           2PE
4002 FOR J=1 TO N
4003 LET Y(J)=Q((J+2),3)
4004 LET P(J,1)=Q((J+1),3)
4005 LET P(J,2)=Q(J,3)
4010 NEXT J
4015 GOSUB 987
4020 GOSUB 1000
4025 GOSUB 971
4030 GOSUB 890
4035 PRINT A(1),A(2)
4040 LET M=3
4045 RETURN
9999 END
```

```
01234567890123456789    ** RSX-11M V3.2 **    [113,1]PHI     - NO PAGE LIMIT
01234567890123456789    ** RSX-11M V3.2 **    FORM #0 - NORMAL HARDWARE FORMS
01234567890123456789    ** RSX-11M V3.2 **    NO IMPLIED FORM FEED
01234567890123456789    ** RSX-11M V3.2 **    DP0:[113,1]PHI.BAS;1
```

```
[[[[[[        11        11        333333              11
[[[[[[        11        11        333333              11
[[          1111      1111      33      33          1111
[[          1111      1111      33      33          1111
[[            11        11              33            11
[[            11        11              33            11
[[            11        11            33      ;;;;    11
[[            11        11            33      ;;;;    11
[[            11        11              33    ;;;;    11
[[            11        11              33    ;;;;    11
[[            11        11      33      33      ;;    11
[[            11        11      33      33      ;;    11
[[[[[[    111111    111111        333333      ;;    111111
[[[[[[    111111    111111        333333      ;;    111111
```

```
PPPPPPPP    HH      HH    IIIIII
PPPPPPPP    HH      HH    IIIIII
PP      PP  HH      HH      II
PP      PP  HH      HH      II
PP      PP  HH      HH      II
PP      PP  HH      HH      II
PPPPPPPP    HHHHHHHHHH      II
PPPPPPPP    HHHHHHHHHH      II
PP          HH      HH      II
PP          HH      HH      II
PP          HH      HH      II
PP          HH      HH      II
PP          HH      HH    IIIIII
PP          HH      HH    IIIIII
```


```
01234567890123456789    ** RSX-11M V3.2 **    [113,1]PHI     - NO PAGE LIMIT
01234567890123456789    ** RSX-11M V3.2 **    FORM #0 - NORMAL HARDWARE FORMS
01234567890123456789    ** RSX-11M V3.2 **    NO IMPLIED FORM FEED
01234567890123456789    ** RSX-11M V3.2 **    DP0:[113,1]PHI.BAS;1
```

```
499 REM ****************************************************************
500 REM *  SUBROUTINE  PHI                                             *
501 REM *  THIS COMPUTES THE STATE TRANSITION MATRIX FOR GYRO          *
502 REM ****************************************************************
503 LET Q=SQR(C(1,3)*C(1,3)+C(2,3)*C(2,3)+C(3,3)*C(3,3))
504 LET A=COS(Q*T)
505 LET B=SIN(Q*T)
510 LET Z(1,1)=A+C(1,3)*C(1,3)*(1-A)/(Q*Q)
511 LET Z(1,2)=C(1,3)*C(2,3)*(1-A)/(Q*Q)+C(3,3)*B/Q
512 LET Z(1,3)=C(1,3)*C(3,3)*(1-A)/(Q*Q)-C(2,3)*B/Q
513 LET Z(2,1)=C(1,3)*C(2,3)*(1-A)/(Q*Q)-C(3,3)*B/Q
514 LET Z(2,2)=A+C(2,3)*C(2,3)*(1-A)/(Q*Q)
515 LET Z(2,3)=C(2,3)*C(3,3)*(1-A)/(Q*Q)+C(1,3)*B/Q
516 LET Z(3,1)=C(1,3)*C(3,3)*(1-A)/(Q*Q)+C(2,3)*B/Q
517 LET Z(3,2)=C(2,3)*C(3,3)*(1-A)/(Q*Q)-C(1,3)*B/Q
518 LET Z(3,3)=A+C(3,3)*C(3,3)*(1-A)/(Q*Q)
520 RETURN
```

```
01234567890123456789      ** RSX-11M V3.2 **      [113,1]PTP     - NO PAGE LIMIT
01234567890123456789      ** RSX-11M V3.2 **      FORM #0 - NORMAL HARDWARE FORMS
01234567890123456789      ** RSX-11M V3.2 **      NO IMPLIED FORM FEED
01234567890123456789      ** RSX-11M V3.2 **      DP0:[113,1]PTP.BAS;2
```

```
  [[[[[[         11           11          333333                      11
  [[[[[[         11           11          333333                      11
  [[           1111         1111       33       33                  1111
  [[           1111         1111       33       33                  1111
  [[             11           11                33                    11
  [[             11           11                33                    11
  [[             11           11              33         ,,,,         11
  [[             11           11              33         ,,,,         11
  [[             11           11                33       ,,,,         11
  [[             11           11                33       ,,,,         11
  [[             11           11       33       33         ,,         11
  [[             11           11       33       33         ,,         11
  [[[[[[       111111       111111        333333         ,,         111111
  [[[[[[       111111       111111        333333         ,,         111111
```

```
PPPPPPPP     TTTTTTTTTT   PPPPPPPP
PPPPPPPP     TTTTTTTTTT   PPPPPPPP
PP      PP       TT       PP      PP
PP      PP       TT       PP      PP
PP      PP       TT       PP      PP
PP      PP       TT       PP      PP
PPPPPPPP         TT       PPPPPPPP
PPPPPPPP         TT       PPPPPPPP
PP               TT       PP
PP               TT       PP
PP               TT       PP
PP               TT       PP
PP               TT       PP
PP               TT       PP
```


```
01234567890123456789      ** RSX-11M V3.2 **      [113,1]PTP     - NO PAGE LIMIT
01234567890123456789      ** RSX-11M V3.2 **      FORM #0 - NORMAL HARDWARE FORMS
01234567890123456789      ** RSX-11M V3.2 **      NO IMPLIED FORM FEED
01234567890123456789      ** RSX-11M V3.2 **      DP0:[113,1]PTP.BAS;2
```

```
980 REM ********************************************
981 REM * SUBROUTINE PTP                           *
982 REM * THIS SUBROUTINE COMPUTES T= P(TRANSPOSE)*P *
984 REM ********************************************
985 PRINT "P IS AN NXM MATRIX,  ENTER N,M"
986 INPUT N,M
987 FOR I=1 TO 3
988 FOR J=1 TO 3
989 LET T(I,J)=0
990 NEXT J
991 NEXT I
992 FOR I=1 TO M
993 FOR J=1 TO M
994 FOR K=1 TO N
995 LET T(I,J)=T(I,J)+P(K,I)*P(K,J)
996 NEXT K
997 NEXT J
998 NEXT I
999 RETURN
```

```
01234567890123456789    ** RSX-11M V3.2 **    [113,1]INVERS - NO PAGE LIMIT
01234567890123456789    ** RSX-11M V3.2 **    FORM #0 - NORMAL HARDWARE FORMS
01234567890123456789    ** RSX-11M V3.2 **    NO IMPLIED FORM FEED
01234567890123456789    ** RSX-11M V3.2 **    DP0:[113,1]INVERS.BAS;1
```

```
  [[[[[[         11           11          333333                      11
  [[[[[[         11           11          333333                      11
  [[           1111         1111        33      33                  1111
  [[           1111         1111        33      33                  1111
  [[             11           11                33                    11
  [[             11           11                33                    11
  [[             11           11              33         ,,,,         11
  [[             11           11              33         ,,,,         11
  [[             11           11                33       ,,,,         11
  [[             11           11                33       ,,,,         11
  [[             11           11        33      33         ,,         11
  [[             11           11        33      33         ,,         11
  [[[[[[       111111       111111        333333         ,,         111111
  [[[[[[       111111       111111        333333         ,,         111111
```

```
  IIIIII     NN       NN   VV      VV   EEEEEEEEEE   RRRRRRRR       SSSSSSSS
  IIIIII     NN       NN   VV      VV   EEEEEEEEEE   RRRRRRRR       SSSSSSSS
    II       NN       NN   VV      VV   EE           RR      RR   SS
    II       NN       NN   VV      VV   EE           RR      RR   SS
    II       NNNN     NN   VV      VV   EE           RR      RR   SS
    II       NNNN     NN   VV      VV   EE           RR      RR   SS
    II       NN  NN   NN   VV      VV   EEEEEEEE     RRRRRRRR       SSSSSS
    II       NN  NN   NN   VV      VV   EEEEEEEE     RRRRRRRR       SSSSSS
    II       NN     NNNN   VV      VV   EE           RR  RR               SS
    II       NN     NNNN   VV      VV   EE           RR  RR               SS
    II       NN       NN     VV  VV     EE           RR    RR             SS
    II       NN       NN     VV  VV     EE           RR    RR             SS
  IIIIII     NN       NN       VV       EEEEEEEEEE   RR      RR   SSSSSSSS
  IIIIII     NN       NN       VV       EEEEEEEEEE   RR      RR   SSSSSSSS
```


```
01234567890123456789    ** RSX-11M V3.2 **    [113,1]INVERS - NO PAGE LIMIT
01234567890123456789    ** RSX-11M V3.2 **    FORM #0 - NORMAL HARDWARE FORMS
01234567890123456789    ** RSX-11M V3.2 **    NO IMPLIED FORM FEED
01234567890123456789    ** RSX-11M V3.2 **    DP0:[113,1]INVERS.BAS;1
```

```
909 REM ***********************************************************
910 REM *   SUBROUTINE INVERS                                     *
911 REM *   THIS SUBROUTINE COMPUTES V=INVERSE OF T; T IS 3X3     *
912 REM *   SUBROUTINE CALLS ADJNT AND DTRMNT                     *
913 REM ***********************************************************
914 GOSUB 953
915 GOSUB 930
916 FOR I=1 TO 3
917 FOR J=1 TO 3
918 LET V(I,J)=U(I,J)/D
919 NEXT J
920 NEXT I
925 RETURN
```

```
01234567890123456789     ** RSX-11M V3.2 **     [113,1]ADJNT  - NO PAGE LIMIT
01234567890123456789     ** RSX-11M V3.2 **     FORM #0 - NORMAL HARDWARE FORMS
01234567890123456789     ** RSX-11M V3.2 **     NO IMPLIED FORM FEED
01234567890123456789     ** RSX-11M V3.2 **     DP0:[113,1]ADJNT.BAS;2
```

```
 [[[[[[       11          11         333333                  11
 [[[[[[       11          11         333333                  11
 [[         1111        1111       33      33              1111
 [[         1111        1111       33      33              1111
 [[           11          11               33                11
 [[           11          11               33                11
 [[           11          11             33       ;;;;       11
 [[           11          11             33       ;;;;       11
 [[           11          11               33     ;;;;       11
 [[           11          11               33     ;;;;       11
 [[           11          11       33      33       ;;       11
 [[           11          11       33      33       ;;       11
 [[[[[[     111111      111111       333333       ;;       111111
 [[[[[[     111111      111111       333333       ;;       111111
```

```
   AAAAAA      DDDDDDDD               JJ   NN       NN   TTTTTTTTTT
   AAAAAA      DDDDDDDD               JJ   NN       NN   TTTTTTTTTT
 AA      AA    DD      DD             JJ   NN       NN       TT
 AA      AA    DD      DD             JJ   NN       NN       TT
 AA      AA    DD      DD             JJ   NNNN     NN       TT
 AA      AA    DD      DD             JJ   NNNN     NN       TT
 AA      AA    DD      DD             JJ   NN  NN   NN       TT
 AA      AA    DD      DD             JJ   NN  NN   NN       TT
 AAAAAAAAAA    DD      DD   JJ        JJ   NN    NNNN        TT
 AAAAAAAAAA    DD      DD   JJ        JJ   NN    NNNN        TT
 AA      AA    DD      DD   JJ        JJ   NN       NN       TT
 AA      AA    DD      DD   JJ        JJ   NN       NN       TT
 AA      AA    DDDDDDDD       JJJJJJ       NN       NN       TT
 AA      AA    DDDDDDDD       JJJJJJ       NN       NN       TT
```


```
01234567890123456789     ** RSX-11M V3.2 **     [113,1]ADJNT  - NO PAGE LIMIT
01234567890123456789     ** RSX-11M V3.2 **     FORM #0 - NORMAL HARDWARE FORMS
01234567890123456789     ** RSX-11M V3.2 **     NO IMPLIED FORM FEED
01234567890123456789     ** RSX-11M V3.2 **     DP0:[113,1]ADJNT.BAS;2
```

```
930 REM ***************************************************************
931 REM *   SUBROUTINE  ADJNT                                         *
932 REM *   THIS SUBROUTINE COMPUTES U=ADJOINT(T)                      *
933 REM ***************************************************************
936 LET U(1,1)=T(2,2)*T(3,3)-T(3,2)*T(2,3)
937 LET U(2,1)=T(3,1)*T(2,3)-T(2,1)*T(3,3)
938 LET U(3,1)=T(2,1)*T(3,2)-T(3,1)*T(2,2)
939 LET U(1,2)=T(3,2)*T(1,3)-T(1,2)*T(3,3)
940 LET U(2,2)=T(1,1)*T(3,3)-T(3,1)*T(1,3)
941 LET U(3,2)=T(3,1)*T(1,2)-T(1,1)*T(3,2)
942 LET U(1,3)=T(1,2)*T(2,3)-T(2,2)*T(1,3)
943 LET U(2,3)=T(2,1)*T(1,3)-T(1,1)*T(2,3)
944 LET U(3,3)=T(1,1)*T(2,2)-T(2,1)*T(1,2)
945 RETURN
```

```
01234567890123456789     ** RSX-11M V3.2 **     [113,1]DTRMNT - NO PAGE LIMIT
01234567890123456789     ** RSX-11M V3.2 **     FORM #0 - NORMAL HARDWARE FORMS
01234567890123456789     ** RSX-11M V3.2 **     NO IMPLIED FORM FEED
01234567890123456789     ** RSX-11M V3.2 **     DPO:[113,1]DTRMNT.BAS;2
```

```
  [[[[[[        11          11         333333                    11
  [[[[[[        11          11         333333                    11
  [[          1111        1111       33      33                1111
  [[          1111        1111       33      33                1111
  [[            11          11               33                  11
  [[            11          11               33                  11
  [[            11          11             33        ,,,,          11
  [[            11          11             33        ,,,,          11
  [[            11          11               33      ,,,,          11
  [[            11          11               33      ,,,,          11
  [[            11          11       33      33        ,,          11
  [[            11          11       33      33        ,,          11
  [[[[[[      111111      111111       333333        ,,          111111
  [[[[[[      111111      111111       333333        ,,          111111
```

```
DDDDDDDD      TTTTTTTTTT    RRRRRRRR      MM      MM    NN      NN    TTTTTTTTTT
DDDDDDDD      TTTTTTTTTT    RRRRRRRR      MM      MM    NN      NN    TTTTTTTTTT
DD      DD        TT        RR      RR    MMMM  MMMM    NN      NN        TT
DD      DD        TT        RR      RR    MMMM  MMMM    NN      NN        TT
DD      DD        TT        RR      RR    MM  MM  MM    NNNN    NN        TT
DD      DD        TT        RR      RR    MM  MM  MM    NNNN    NN        TT
DD      DD        TT        RRRRRRRR      MM      MM    NN  NN  NN        TT
DD      DD        TT        RRRRRRRR      MM      MM    NN  NN  NN        TT
DD      DD        TT        RR  RR        MM      MM    NN    NNNN        TT
DD      DD        TT        RR  RR        MM      MM    NN    NNNN        TT
DD      DD        TT        RR    RR      MM      MM    NN      NN        TT
DD      DD        TT        RR    RR      MM      MM    NN      NN        TT
DDDDDDDD          TT        RR      RR    MM      MM    NN      NN        TT
DDDDDDDD          TT        RR      RR    MM      MM    NN      NN        TT
```


```
01234567890123456789     ** RSX-11M V3.2 **     [113,1]DTRMNT - NO PAGE LIMIT
01234567890123456789     ** RSX-11M V3.2 **     FORM #0 - NORMAL HARDWARE FORMS
01234567890123456789     ** RSX-11M V3.2 **     NO IMPLIED FORM FEED
01234567890123456789     ** RSX-11M V3.2 **     DPO:[113,1]DTRMNT.BAS;2
```

```
953 REM ****************************************************************
954 REM *  SUBROUTINE DTRMNT                                             *
955 REM *  THIS SUBROUTINE COMPUTES D=DET(T)                             *
956 REM ****************************************************************
957 LET D=T(1,1)*(T(2,2)*T(3,3)-T(3,2)*T(2,3))
958 LET D=D+T(1,2)*(T(3,1)*T(2,3)-T(2,1)*T(3,3))
959 LET D=D+T(1,3)*(T(2,1)*T(3,2)-T(3,1)*T(2,2))
960 RETURN
```

01234567890123456789 ** RSX-11M V3.2 ** [113,1]PTY - NO PAGE LIMIT
01234567890123456789 ** RSX-11M V3.2 ** FORM #0 - NORMAL HARDWARE FORM
01234567890123456789 ** RSX-11M V3.2 ** NO IMPLIED FORM FEED
01234567890123456789 ** RSX-11M V3.2 ** DP0:[113,1]PTY.BAS;2

```
[[[[[[        11          11          333333                 11
[[[[[[        11          11          333333                 11
[[          1111        1111        33      33             1111
[[          1111        1111        33      33             1111
[[            11          11                33               11
[[            11          11                33               11
[[            11          11              33      ,,,,       11
[[            11          11              33      ,,,,       11
[[            11          11                33    ,,,,       11
[[            11          11                33    ,,,,       11
[[            11          11        33      33      ,,       11
[[            11          11        33      33      ,,       11
[[[[[[      111111      111111        333333      ,,       111111
[[[[[[      111111      111111        333333      ,,       111111
```

```
PPPPPPPP      TTTTTTTTTT    YY        YY
PPPPPPPP      TTTTTTTTTT    YY        YY
PP      PP        TT        YY        YY
PP      PP        TT        YY        YY
PP      PP        TT          YY    YY
PP      PP        TT          YY    YY
PPPPPPPP          TT            YY
PPPPPPPP          TT            YY
PP                TT            YY
PP                TT            YY
PP                TT            YY
PP                TT            YY
PP                TT            YY
PP                TT            YY
```

01234567890123456789 ** RSX-11M V3.2 ** [113,1]PTY - NO PAGE LIMIT
01234567890123456789 ** RSX-11M V3.2 ** FORM #0 - NORMAL HARDWARE FORMS
01234567890123456789 ** RSX-11M V3.2 ** NO IMPLIED FORM FEED
01234567890123456789 ** RSX-11M V3.2 ** DP0:[113,1]PTY.BAS;2

```
964 REM *****************************************************************
965 REM * SUBROUTINE PTY                                                *
966 REM *  THIS SUBROUTINE COMPUTES O= P(TRANSPOSE *Y WHERE P IS NXM    *
967 REM *  AND Y IS NX1                                                 *
968 REM *****************************************************************
969 PRINT "Y  IS NX1 ENTER N"
970 INPUT N
971 FOR I=1 TO M
972 LET O(I)=0
973 NEXT I
974 FOR I=1 TO M
975 FOR J=1 TO N
976 LET O(I)=O(I)+P(J,I)*Y(J)
977 NEXT J
978 NEXT I
979 RETURN
```

```
01234567890123456789     ** RSX-11M V3.2 **     [113,1]PTPPTY - NO PAGE LIMIT
01234567890123456789     ** RSX-11M V3.2 **     FORM #0 - NORMAL HARDWARE FORMS
01234567890123456789     ** RSX-11M V3.2 **     NO IMPLIED FORM FEED
01234567890123456789     ** RSX-11M V3.2 **     DP0:[113,1]PTPPTY.BAS;2
```

```
  [[[[[[          11          11          333333                  11
  [[[[[[          11          11          333333                  11
  [[            1111        1111        33      33              1111
  [[            1111        1111        33      33              1111
  [[              11          11                33                11
  [[              11          11                33                11
  [[              11          11              33      ;;;;        11
  [[              11          11              33      ;;;;        11
  [[              11          11                33    ;;;;        11
  [[              11          11                33    ;;;;        11
  [[              11          11        33      33      ;;        11
  [[              11          11        33      33      ;;        11
  [[[[[[        111111      111111        333333      ;;        111111
  [[[[[[        111111      111111        333333      ;;        111111
```

```
PPPPPPPP      TTTTTTTTTT    PPPPPPPP      PPPPPPPP      TTTTTTTTTT    YY      YY
PPPPPPPP      TTTTTTTTTT    PPPPPPPP      PPPPPPPP      TTTTTTTTTT    YY      YY
PP      PP        TT        PP      PP    PP      PP        TT        YY      YY
PP      PP        TT        PP      PP    PP      PP        TT        YY      YY
PP      PP        TT        PP      PP    PP      PP        TT          YY  YY
PP      PP        TT        PP      PP    PP      PP        TT          YY  YY
PPPPPPPP          TT        PPPPPPPP      PPPPPPPP          TT            YY
PPPPPPPP          TT        PPPPPPPP      PPPPPPPP          TT            YY
PP                TT        PP            PP                TT            YY
PP                TT        PP            PP                TT            YY
PP                TT        PP            PP                TT            YY
PP                TT        PP            PP                TT            YY
PP                TT        PP            PP                TT            YY
PP                TT        PP            PP                TT            YY
```


```
01234567890123456789     ** RSX-11M V3.2 **     [113,1]PTPPTY - NO PAGE LIMIT
01234567890123456789     ** RSX-11M V3.2 **     FORM #0 - NORMAL HARDWARE FORMS
01234567890123456789     ** RSX-11M V3.2 **     NO IMPLIED FORM FEED
01234567890123456789     ** RSX-11M V3.2 **     DP0:[113,1]PTPPTY.BAS;2
```

```
879 REM ***************************************************
890 REM *  SUBROUTINE PTPPTY                              *
891 REM *  THIS SUBROUTINE COMPUTES A= V*O ; V IS MXM  O IS MX1*
892 REM ***************************************************
893 FOR I=1 TO M
894 LET A(I)=0
895 NEXT I
896 FOR I=1 TO M
897 FOR J=1 TO M
898 LET A(I)=A(I)+V(I,J)*O(J)
899 NEXT J
900 NEXT I
905 RETURN
```

```
01234567890123456789    ** RSX-11M V3.2 **    [113,1]INVERT - NO PAGE LIMIT
01234567890123456789    ** RSX-11M V3.2 **    FORM #0 - NORMAL HARDWARE FORMS
01234567890123456789    ** RSX-11M V3.2 **    NO IMPLIED FORM FEED
01234567890123456789    ** RSX-11M V3.2 **    DP0:[113,1]INVERT.BAS;1



[[[[[[         11           11         333333                      11
[[[[[[         11           11         333333                      11
[[           1111         1111       33      33                  1111
[[           1111         1111       33      33                  1111
[[             11           11               33                    11
[[             11           11               33                    11
[[             11           11             33         ,,,,         11
[[             11           11             33         ,,,,         11
[[             11           11               33       ,,,,         11
[[             11           11               33       ,,,,         11
[[             11           11       33      33         ,,         11
[[             11           11       33      33         ,,         11
[[[[[[       111111       111111       333333         ,,         111111
[[[[[[       111111       111111       333333         ,,         111111



IIIIII     NN      NN   VV      VV   EEEEEEEEEE   RRRRRRRR     TTTTTTTTTT
IIIIII     NN      NN   VV      VV   EEEEEEEEEE   RRRRRRRR     TTTTTTTTTT
  II       NN      NN   VV      VV   EE           RR      RR       TT
  II       NN      NN   VV      VV   EE           RR      RR       TT
  II       NNNN    NN   VV      VV   EE           RR      RR       TT
  II       NNNN    NN   VV      VV   EE           RR      RR       TT
  II       NN  NN  NN   VV      VV   EEEEEEEE     RRRRRRRR         TT
  II       NN  NN  NN   VV      VV   EEEEEEEE     RRRRRRRR         TT
  II       NN    NNNN   VV      VV   EE           RR  RR           TT
  II       NN    NNNN   VV      VV   EE           RR  RR           TT
  II       NN      NN     VV  VV     EE           RR    RR         TT
  II       NN      NN     VV  VV     EE           RR    RR         TT
IIIIII     NN      NN       VV       EEEEEEEEEE   RR      RR       TT
IIIIII     NN      NN       VV       EEEEEEEEEE   RR      RR       TT
```


```
01234567890123456789    ** RSX-11M V3.2 **    [113,1]INVERT - NO PAGE LIMIT
01234567890123456789    ** RSX-11M V3.2 **    FORM #0 - NORMAL HARDWARE FORMS
01234567890123456789    ** RSX-11M V3.2 **    NO IMPLIED FORM FEED
01234567890123456789    ** RSX-11M V3.2 **    DP0:[113,1]INVERT.BAS;1
```

```
1000 REM *****************************************************************
1001 REM *   SUBROUTINE INVERT                                           *
1002 REM *   THIS SUBROUTINE COMPUTES  V=INVERSE OF T  T IS (2X2)        *
1003 REM *****************************************************************
1010 LET D=T(1,1)*T(2,2)-T(1,2)*T(2,1)
1011 LET V(1,1)=T(2,2)/D
1012 LET V(1,2)=-T(2,1)/D
1013 LET V(2,1)=-T(1,2)/D
1014 LET V(2,2)=T(1,1)/D
1015 RETURN
```

END

FILMED

11-85

DTIC